Paxilline inhibits BK channels by an almost exclusively closed-channel block mechanism

Yu Zhou and Christopher J. Lingle

Department of Anesthesiology, Washington University School of Medicine, St. Louis, MO 63110

Paxilline, a tremorogenic fungal alkaloid, potently inhibits large conductance Ca^{2+}- and voltage-activated K^+ (BK)-type channels, but little is known about the mechanism underlying this inhibition. Here we show that inhibition is inversely dependent on BK channel open probability (Po), and is fully relieved by conditions that increase Po, even in the constant presence of paxilline. Manipulations that shift BK gating to more negative potentials reduce inhibition by paxilline in accordance with the increase in channel Po. Measurements of Po times the number of channels at negative potentials support the idea that paxilline increases occupancy of closed states, effectively reducing the closed–open equilibrium constant, L(0). Gating current measurements exclude an effect of paxilline on voltage sensors. Steady-state inhibition by multiple paxilline concentrations was determined for four distinct equilibration conditions, each with a distinct Po. The IC_{50} for paxilline shifted from around 10 nM when channels were largely closed to near 10 µM as maximal Po was approached. Model-dependent analysis suggests a mechanism of inhibition in which binding of a single paxilline molecule allosterically alters the intrinsic L(0) favoring occupancy of closed states, with affinity for the closed conformation being >500-fold greater than affinity for the open conformation. The rate of inhibition of closed channels was linear up through 2 µM paxilline, with a slope of $2 \times 10^6 \, M^{-1} s^{-1}$. Paxilline inhibition was hindered by either the bulky cytosolic blocker, bbTBA, or by concentrations of cytosolic sucrose that hinder ion permeation. However, paxilline does not hinder MTSET modification of the inner cavity residue, A313C. We conclude that paxilline binds more tightly to the closed conformation, favoring occupancy of closed-channel conformations, and propose that it binds to a superficial position near the entrance to the central cavity, but does not hinder access of smaller molecules to this cavity.

INTRODUCTION

Since the early days of investigation of ion channel function to the present day in which functional studies of ion channels are also guided by structural information, molecules that inhibit ion channels continue to be essential tools for probing state-dependent conformational changes in binding-site accessibility. For potassium channels (K^+ channels), some of the earliest work with channel blockers insightfully established that state-dependent conformational changes on the cytosolic side of voltage-dependent K^+ channels are required to allow charged quaternary blockers to reach their blocking position within the pore (Armstrong, 1969; Armstrong and Hille, 1972; Choi et al., 1991). Furthermore, for many Kv channels, channel closure can only occur after exit of the blocker from its blocking position (Armstrong and Hille, 1972; Choi et al., 1993). This idea that there is gated access to the permeation pathway from the cytosolic side of K^+ channels was subsequently born out in structures of K^+ channels (Doyle et al., 1998; Long et al.,

2005; Uysal et al., 2009). First, in closed K^+ channels, the so-called crossing of the S6 helices provides a physical barrier to access of small molecules to an inner aqueous cavity preceding the selectivity filter. Second, in open K^+ channels, separation of the S6 helices creates an aperture (Perozo et al., 1999) that allows access not only of permeant ions but also of quaternary blockers (Lenaeus et al., 2005) and peptides (Zhou et al., 2001) to positions within the inner cavity. Together, these types of functional and structural tests have provided a compelling picture of a category of channel inhibition that exclusively involves open-channel block; that is, binding sites for particular blockers only become available when the channel is open. However, ion channel inhibition can also occur by a variety of other mechanisms, which can also be informative about channel function and its structural components. One particularly rich source of interesting channel blockers are naturally occurring toxins.

Evolutionary pressures for species to optimize their survival have resulted in a vast, useful, and only partially exploited array of naturally occurring compounds that

The Rockefeller University Press $30.00
J. Gen. Physiol. Vol. 144 No. 5   415–440
www.jgp.org/cgi/doi/10.1085/jgp.201411259

415

may kill or incapacitate prey or limit predation (Bush et al., 1997; Han et al., 2008; Liang, 2008). Such compounds often target ion channels, and the high selectivity and strong affinity for particular ion channels have proven of enormous value for the identification of particular subtypes of ion channels and their physiological roles. Many such toxins are thought to act simply by binding to the extracellular face of an ion channel, perhaps in a largely state-independent fashion, thereby occluding ion permeation or preventing channel openings. This would include toxins such as tetrodotoxin acting on Na^+ channels (Narahashi et al., 1964, 1967), charybdotoxin (ChTX) acting on large conductance Ca^{2+}- and voltage-activated K^+ (BK)-type K^+ channels (Smith et al., 1986; Anderson et al., 1988; MacKinnon and Miller, 1988), and agitoxin acting on voltage-dependent K^+ channels (Gross and MacKinnon, 1996). Recent structural work has now specifically defined the complex of ChTX in association with the Kv2.1 paddle-Kv1.2 chimeric channel (Banerjee et al., 2013). Over the past several years, another category of naturally occurring toxin has been identified that selectively targets voltage-sensor domains of K^+ channels, inhibiting channels by stabilizing voltage-sensor domains in resting conformations (Swartz and MacKinnon, 1997a,b; Lee and MacKinnon, 2004; Milescu et al., 2009; Wang et al., 2011). The ability of toxins to target not only specific ion channels but also specific functional domains of ion channels suggests that additional channel inhibitory mechanisms may remain to be revealed.

Some channel-blocking agents, for which detailed mechanistic information remains incomplete, have been termed "allosteric blockers" or "closed-channel blockers." Such descriptions simply imply that a binding site and mechanism exist, different from direct physical occlusion of the permeation pathway, that maintains channels in nonconducting states. The voltage-sensor toxins, in fact, would fall in this category: they maintain voltage sensors in resting states, thereby allosterically preventing channel opening. However, in most cases for which a channel inhibitory mechanism has been termed allosteric, the specific details of how drug binding is related to channel inhibition remain unclear. One example of such a poorly understood allosteric blocking mechanism is the inhibition of BK-type K^+ channels by the naturally occurring fungal alkaloid, paxilline (Knaus et al., 1994; Sanchez and McManus, 1996; Imlach et al., 2009). The BK channel is a particularly attractive target for elucidation of an allosteric blocking mechanism, because the well-developed framework that describes allosteric regulation of BK channels (Horrigan and Aldrich, 2002) allows one to assess which part of the BK gating apparatus may be influenced by a compound.

Paxilline is one of a variety of fungal indole alkaloids (Cole and Cox, 1981; Knaus et al., 1994; Imlach et al.,

2009) that are potent nonpeptidergic blockers of BK channels, generally acting at low nanomolar concentrations (Knaus et al., 1994; Imlach et al., 2009). Because some BK channels containing particular auxiliary β subunits exhibit resistance to block by the BK-blocking scorpion toxins, iberiotoxin and ChTX (Xia et al., 1999; Meera et al., 2000; Xia et al., 2000), paxilline, as a more general BK inhibitor, is often used in tests of physiological roles of BK channels (Shao et al., 1999; Raffaelli et al., 2004; Tammaro et al., 2004; Essin et al., 2009). Although inhibition by paxilline has been termed allosteric and shows relief by elevations of Ca^{2+} (Sanchez and McManus, 1996), the mechanism and site of action of the lipophilic paxilline are unknown. Recently, we observed that mutation of the so-called hinge glycine position (G311) in the S6 helix thought to line the BK channel inner cavity totally abolishes paxilline inhibition (Zhou et al., 2010). This suggests that paxilline block is associated in some way with the BK pore-gate domain, perhaps dependent in some way on the conformational status of the inner pore. Here, we establish that paxilline inhibition can best be viewed as an allosteric effect on the BK channel closed–open (C-O) equilibrium, stabilizing channels in closed conformations, while having no discernible direct blocking effect on open BK channels and no effect on voltage sensors. Occupancy of the paxilline-binding site does not directly occlude ion permeation, but binding shifts the channel C-O equilibrium, resulting in stabilization of channels in closed states.

MATERIALS AND METHODS

General methods

Oocyte preparation, handling of RNA, and electrophysiological methods used here were identical to those described in other recent papers from this laboratory (Tang et al., 2009; Zhou et al., 2010). All experiments used excised inside-out patches in which solution exchange at the pipette tip was accomplished with a fast perfusion stepper system (SF-77B; Warner Instruments). Pipettes were typically 1–2 MΩ, except for patches used for open probability (Po) times the number of channels (NPo) or gating current measurements, and were coated with Sylgard (Sylgard 184; Corning) before heat polishing. Gigaohm seals were formed while the oocytes were bathed in frog Ringer's solution (mM: 115 NaCl, 2.5 KCl, 1.8 CaCl$_2$, and 10 HEPES, pH 7.4). After patch excision, the pipette tip was moved into flowing test solutions. The pipette solution (bathing the extracellular membrane face) contained (mM): 140 K-methanesulfonate, 20 KOH, 10 HEPES, and 2 MgCl$_2$, pH 7.0. The composition of the solution used to bathe the cytoplasmic face of patch membranes was (mM): 140 K-methanesulfonate, 20 KOH, and 10 HEPES, with pH adjusted to 7.0. For 0 Ca^{2+}, the solution also contained 5 mM EGTA; for 10 µM Ca^{2+}, it contained 5 mM HEDTA; and for 100 or 300 µM Ca^{2+}, no Ca^{2+} buffer was included. For 10 µM Ca^{2+}, the solution was titrated with a Ca^{2+}-methanesulfonate solution to obtain the desired Ca^{2+} concentration (Zhang et al., 2001), as defined with a Ca^{2+}-sensitive electrode calibrated with commercial Ca^{2+} solutions (WPI). Measurements and fitting of current recordings were accomplished either with Clampfit (Molecular Devices) or with programs written in this

laboratory. Experiments were performed at room temperature (∼22–25°C).

NPo measurements. For determination of NPo at negative potentials, patches were pulled from oocytes expressing large numbers of BK channels. Openings were determined with the threshold-based single-channel search function of Clampfit 9, and total amplitude histograms were generated from the current records. A fit of a Gaussian function to the total amplitude histograms was used to estimate NPo under various concentrations of paxilline.

Gating current measurements. Gating currents were recorded from inside-out macropatches (10–20 µM in diameter). The pipette solution contained (mM):127 tetraethylammonium hydroxide, 125 methanesulfonic acid, 2 $MgCl_2$, and 10 HEPES, pH 7.0. The internal solution contained (mM): 141 NMDG, 135 methanesulfonic acid, 10 HEPES, and 5 EGTA, pH 7.0. Voltage commands were filtered at 20 kHz with an eight-pole Bessel filter (Frequency Devices) to avoid saturation by fast capacitive transients (Horrigan and Aldrich, 1999). Gating currents were filtered at 10 kHz with the internal filter of the Axopatch and sampled at 100 kHz. Capacitive transients and leak currents were subtracted using a P/5 protocol with a holding potential of −80 mV.

Constructs. The *mSlo1* construct containing the coding region of mSlo1 (GenBank accession no. NM_010610; provided by L. Salkoff, Washington University School of Medicine, St. Louis, MO) was subcloned into the pXMX oocyte expression vector (Tang et al., 2009). For experiments involving MTS reagents, the control Slo1 construct contained the C430S mutation, which abolishes a shift in gating produced in WT Slo1 channels by MTS reagents (Zhang and Horrigan, 2005). The A313C and A316C mutations were as described previously (Zhou et al., 2011).

Estimates of block parameters. Both the onset of block and recovery from block by paxilline occur slowly, with time constants on the order of seconds. Furthermore, block by paxilline exhibits no voltage dependence during the time course of typical voltage steps used to define activation of conductance as a function of voltage. Thus, as will be more strongly developed in the Results, the fractional block under any condition reflects the state dependence of paxilline block established at the specific holding potential and Ca^{2+} concentration before any change in activation voltage. Together, we term the particular holding potential and Ca^{2+} concentration during which paxilline block equilibrates as the "equilibration condition." We consider three general schemes of state-dependent block. In Scheme 1, paxilline binds to both open and closed BK channels, but paxilline-bound open BK channels are able to conduct current, with inhibition resulting from stabilization of the paxilline-bound closed state. This corresponds to allosteric regulation of the BK C-O intrinsic gating equilibrium, governed by coupling constant, E_p, representing the change in the C-O equilibrium when paxilline is bound (binding equilibrium constant, K_p). In Scheme 2, paxilline only binds to closed BK channels, thereby increasing occupancy in closed states. Scheme 2 is a limiting case of Scheme 1, with coupling constant E_p <<< 1. In Scheme 3, paxilline binds and blocks both open and closed BK channels. As we will establish, the paxilline-blocking equilibrium is essentially unchanged during test sequences that are used to define G-V curves. Therefore, for any scheme, the G-V curves generated from brief test steps in the presence of paxilline will reflect only the contributions of the unblocked channels available at any given equilibration condition. Thus, a G-V curve in the presence of paxilline will be defined by
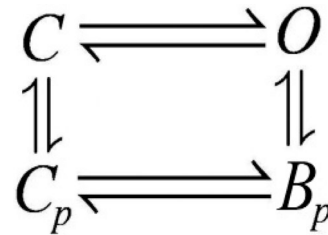
the control G-V curves, scaled by the fraction of unblocked channels (f_{un}) at any given equilibration potential. For Scheme 1, $f_{un}(pax) = (O + C + O_p)/(O + C + O_p + C_p)$. For Scheme 2 with no open-blocked channels, $f_{un}(pax) = (O + C)/(O + C + C_p)$. For Scheme 3, the fraction of unblocked channels is given by: $f_{un}(pax) = (O + C)/(O + C + C_p + B_p)$.
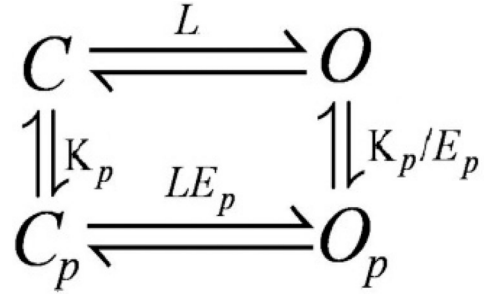
(Scheme 1)
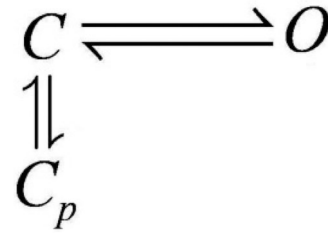
(Scheme 2)

(Scheme 3)

As in previous work (Tang et al., 2009), control G-V curves were fit based on a standard allosteric model of BK channel activation (Horrigan and Aldrich, 2002). Specifically, we describe the control G-V with

$$Po(V) = \frac{1}{1 + \bar{L}},$$

where

$$\bar{L} = \left(\frac{1}{L}\right)\left(\frac{1 + J + K + JKE}{1 + JD + KC + JDKCE}\right)^4,$$

where L, K, and J represent the C-O equilibrium, Ca^{2+}-binding equilibrium, and the voltage-sensor equilibrium, respectively, with D, C, and E representing coupling between J and L, coupling between K and L, and coupling between J and K, respectively. After definition of constants suitable to describe the control G-V

curves, these parameters were then constrained, while parameters for blocking schemes were defined.

Given that no changes in the paxilline-blocking equilibrium occur during the duration of voltage steps used to test BK activation, the predicted dependence of the G-V curve for any scheme in the presence of paxilline will be given by

$$G(V) = \frac{1}{1+\overline{L}} f_{un}(pax).$$

With the paxilline affinity to the closed channel given by K_p, the open-state affinity, $K_{p(o)}$, is K_p/E_p. For Scheme 1, in which the binding of paxilline allosterically regulates the C-O equilibrium constant, L, favoring stabilization of closed states, open channels, although able to bind paxilline, remain conducting with:

$$f_{un}(Pax, hp) = \frac{1+\overline{L_{hp}}+\dfrac{E_p[Pax]}{K_p}}{1+\overline{L_{hp}}+\dfrac{E_p[Pax]}{K_p}+\overline{L_{hp}}\dfrac{[Pax]}{K_p}}, \qquad (1)$$

where $\overline{L_{(hp)}}$ is as defined above but for the equilibrium conditions defined by the holding potential. Scheme 2, in which paxilline does not bind to open channels, is described by Eq. 1 with $E_p = 0$, such that:

$$f_{un}(Pax, hp) = \frac{1+\overline{L_{hp}}}{1+\overline{L_{hp}}+\overline{L_{hp}}\dfrac{[Pax]}{K_p}}. \qquad (2)$$

For Scheme 3, in which paxilline can bind to both open and closed channels and the bound-open channel is nonconducting,

$$f_{un}(Pax, hp) = \frac{1+\overline{L_{hp}}}{1+\overline{L_{hp}}+\dfrac{E_p[Pax]}{K_p}+\overline{L_{hp}}\dfrac{[Pax]}{K_p}}. \qquad (3)$$

Eqs. 1–3 all assume binding of a single paxilline molecule per channel. The possibility that inhibition may be associated with binding of multiple paxilline molecules will be considered in the Results. Under various limiting conditions, some schemes become equivalent. For example, when $E_p \ll 1$ (i.e., $K_p \lll K_{p(o)}$), all three schemes are essentially identical. Furthermore, in Scheme 3, by fixing closed-channel block to very weak binding affinity, Eq. 3 defines fractional unblock in accordance with a standard open-channel block model. The use of the H-A formulation to describe activation is not critical for evaluating paxilline effects on the G-V curves, as a simple Boltzmann description of activation would also suffice. However, the H-A formulation becomes useful when simultaneously fitting inhibition by paxilline over multiple activation conditions (e.g., Figs. 6 E and 7).

For fitting of fractional inhibition by paxilline across multiple conditions, Eqs. 1–3 were adapted in the following way. Under different holding conditions of voltage and Ca^{2+}, the application of paxilline results in some defined reduction of current, reflecting equilibration of channels into nonactivatable, paxilline-bound states. The test steps to positive voltages are then assumed, for Scheme 1, to result in the opening of all channels not in closed-paxilline–bound states. Thus, channels simply in closed states will be activated during the brief test steps. The fraction of unblocked channels at any condition, $f_{un}(Ca^{2+}, V, [Pax])$, is therefore defined by the ratio of I_{pax}/I_{max} at a positive test activation potential. Hence, for Scheme 1, where I_{max} reflects maximal activation,

$$I_{pax}/I_{max} = f_{un}(Ca^{2+}, hp, pax) = \frac{1+\overline{L_{hp}}+\dfrac{E_p[Pax]}{K_p}}{1+\overline{L_{hp}}+\dfrac{E_p[Pax]}{K_p}+\overline{L_{hp}}\dfrac{[Pax]}{K_p}}, \qquad (4)$$

with appropriate changes to accommodate Schemes 2 and 3. For measurement of NPo at a fixed holding potential, only channels in O and paxilline-bound–open states (O_p) would contribute to Po. At the limit of very low Po,

$$NPo_{pax}/NPo_{0\,pax} = \frac{1+\dfrac{E_p[Pax]}{K_p}}{1+\dfrac{[Pax]}{K_p}}, \qquad (5)$$

or, at $E_p \lll 1$,

$$NPo_{pax}/NPo_{0\,pax} = \frac{1}{1+\dfrac{[Pax]}{K_p}}. \qquad (6)$$

Fitting of functions to various datasets was done with a Levenberg–Marquardt nonlinear least-squares fitting algorithm implemented within software developed within this laboratory. Error estimates for fitted parameters represent 90% confidence limits. For all plots, points and error bars show means ± SEM.

Chemicals. Salts and paxilline were obtained from Sigma-Aldrich. The details of the handling of paxilline were as described previously (Zhou et al., 2010). 20-mM stock solutions of paxilline were prepared in 100% DMSO and stored at −20°C. Paxilline-containing physiological solutions were prepared the day of an experiment and only used up to 4 h after preparation. [2-(trimethylammonium)ethyl] MTS bromide (MTSET), 2-aminoethyl MTS (MTSEA), and sodium (2-sulfanoethyl) MTS (MTSES) were obtained from Toronto Research Chemicals.

RESULTS

BK current that gates during partial inhibition by paxilline is indistinguishable from BK current in the absence of paxilline

Previous reports have suggested that paxilline may alter BK G-V curves (Sanchez and McManus, 1996), although this has not been a consistent feature of paxilline action or that of related alkaloids (Imlach et al., 2009, 2011; Zhou et al., 2010). A shift in the G-V curve in the presence of paxilline would suggest that part of paxilline inhibition of BK channels arises from alteration in the BK gating equilibrium during the time of test steps. Because of the challenges posed by slowly acting and slowly reversible blocking drugs, we confined our comparisons to patches in which complete recovery from paxilline inhibition could be achieved. In such cases, we observed that G-V curves generated from BK channels
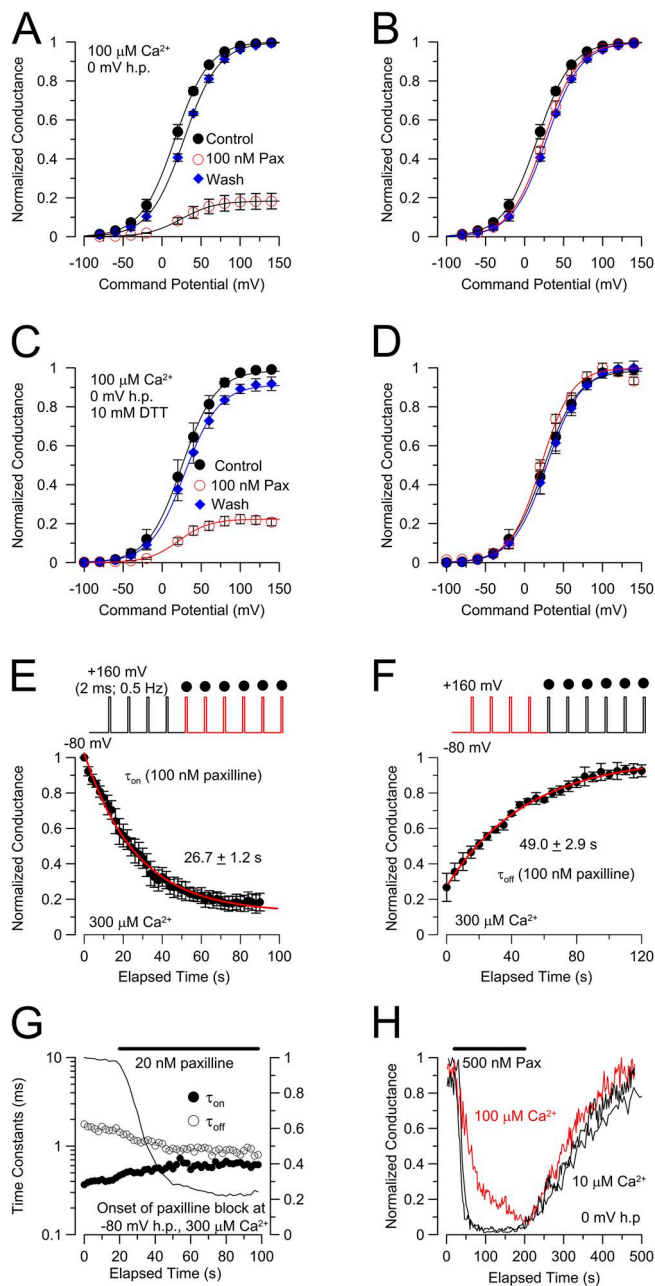
Figure 1. Channels that activate in the presence of paxilline gate with normal voltage dependence and kinetics. (A) G-V curves were normalized to the maximal conductance observed in control saline. Currents were activated with 10 µM cytosolic Ca^{2+} from a holding potential of 0 mV. For prepaxilline, $V_h = 16.31 \pm 0.15$ mV ($z = 0.87 \pm 0.01$ e); in 100 nM paxilline, $V_h = 24.75 \pm 0.13$ mV ($z = 0.86 \pm 0.01$ e); and, after washout of paxilline, $V_h = 28.0 \pm 0.19$ mV ($z = 0.88 \pm 0.01$ e). (B) G-V curves from A were normalized to the fitted maximum for each condition to highlight the lack of G-V shift. (C) G-V curves were generated in the presence and absence of paxilline, but with all solutions containing 10 mM DTT ($n = 7$ patches). For control saline, $V_h = 25.04 \pm 1.2$ mV ($z = 0.86 \pm 0.06$ e); with 50 nM paxilline, $V_h = 21.21 \pm 1.85$ ($z = 0.79 \pm 0.07$ e); and after wash, $V_h = 28.65 \pm 9.0$ ($z = 1.13 \pm 0.05$ e). (D) The same G-V curves in C are normalized to the maximal conductance in each case to highlight their similarity. (E) 2-ms steps to 160 mV were applied at 0.2 Hz to monitor BK activation with 300 µM Ca^{2+}, while holding the patch at −80 mV. The application of 100 nM

---

in inside-out patches studied with symmetrical K$^+$ solutions exhibit no clear shift in the voltage of half-activation during applications of paxilline at concentrations producing >50% inhibition (Fig. 1, A and B). Because of concern that slow gating shifts, perhaps redox dependent (DiChiara and Reinhart, 1997), might appear to underlie a change during prolonged paxilline application, we also examined the effect of paxilline on G-V curves in the constant presence of dithiothreitol (Fig. 1, C and D) without observing any effect. Thus, those BK channels that are activated during brief activation steps in the presence of paxilline appear to open and close with normal voltage and Ca^{2+} dependence. In the Discussion, we point out reasons why apparent shifts in G-V curves might be observed under some conditions based on the features of the paxilline inhibitory mechanism described here.

During the wash-in and wash-out of paxilline, both inhibition (Fig. 1 E) and removal of inhibition (Fig. 1 F) develop over tens of seconds, despite the use of a solution exchange system in which blockade and recovery from inhibition by quaternary ammonium blockers is complete within a few seconds or hundreds of milliseconds (e.g., see Fig. 12). Although it is possible that a slow equilibration of the paxilline concentration at the site of inhibition may contribute to the slow kinetics, it seems likely that the molecular steps involved in the development and recovery from paxilline inhibition are themselves slow (as will be addressed further below). Under such a situation, once a particular blocking equilibrium is established at a given holding condition, brief changes in membrane potential (as in the generation of a G-V curve) would not be expected to appreciably alter the overall block equilibrium. Therefore, although paxilline inhibition does depend inversely on channel Po (see below), under all conditions both the onset and recovery from paxilline inhibition is sufficiently slow, such that brief depolarizations of a few tens of milliseconds will not alter the paxilline block equilibrium established at a given holding condition. As an additional evaluation of the properties of channels activated in the presence of paxilline, we compared the activation and deactivation time course of BK currents in the absence

---

paxilline results in slow diminution of BK current with a time constant (fitted red line) of 9.6 ± 1.1 s. (F) For the same patches as in E, steps to 160 mV with 300 µM Ca^{2+} were used to monitor recovery from paxilline inhibition, with recovery at 300 µM Ca^{2+} at −80 mV with the indicated recovery time constant (red line). (G) For a single patch, BK current activation (closed circles) was monitored at 160 mV and deactivation (open circles) at −80 mV with 300 µM Ca^{2+} before and during the application of 20 nM paxilline, showing that paxilline does not alter the kinetics of channels that open and close in the presence of paxilline. (H) A patch was held at 0 mV and 500 nM paxilline was applied at either of two different Ca^{2+} concentrations (10 or 100 µM). The onset of paxilline block is more rapid with 10 µM Ca^{2+}.

of paxilline and during development of inhibition by paxilline (Fig. 1 G). As inhibition by paxilline develops, neither the activation nor deactivation time constant is altered.

Collectively, these initial tests establish a few features of paxilline inhibition critical to evaluation of later experiments. First, the results show that the BK current that persists during partial inhibition by paxilline gate normally. Second, these results are consistent with the suggestion (Zhou et al., 2010) that the fractional inhibition by paxilline reflects inhibition established at the holding condition or equilibration conditions of the experiment (i.e., voltage and Ca^{2+}). Channels inhibited by paxilline simply do not contribute to the observed currents, and brief depolarizing steps do not result in changes in the paxilline block equilibrium.

Prompted by earlier results (Sanchez and McManus, 1996) indicating that inhibition of BK channels by paxilline is reduced by elevations in Ca^{2+}, we also examined the onset and/or recovery of paxilline inhibition with either 10 or 100 µM Ca^{2+} while holding a patch at 0 mV. The onset of block by 500 nM paxilline was faster and recovery was slower with 10 µM Ca^{2+} compared with 100 µM Ca^{2+} (Fig. 1 H), qualitatively consistent with the earlier observations (Sanchez and McManus, 1996). This result prompted a more detailed examination of the conditions that influence paxilline inhibition presented below.

Inhibition by paxilline varies inversely with steady-state channel Po at the equilibrium condition

To explore further the dependence of paxilline inhibition on Ca^{2+}, we examined the fractional block produced by paxilline on BK channels held under three different equilibration conditions differing in Po: (1) 0 mV, 10 µM Ca^{2+} (Po of ~0.02); (2) −70 mV, 300 µM Ca^{2+} (Po of ~0.07); (3) 0 mV, 300 µM Ca^{2+} (Po of ~0.48). G-V curves were generated for each equilibration condition for control solutions and in both 10 and 100 nM paxilline. For this set of patches, each patch was examined under all three conditions. In each case, paxilline was applied for 4 min to allow equilibration before generation of curves. Recovery from any individual application of paxilline was at least 90%. For the condition of lowest resting Po (Po of <0.02; 0 mV, 10 µM Ca^{2+}), 10 nM paxilline blocked over half the current activated at each voltage, whereas 100 nM paxilline produced essentially complete inhibition (Fig. 2 A). Changing the equilibration condition to 300 µM Ca^{2+} at 0 mV (Po of ~0.48; Fig. 2 B) resulted in a marked reduction in the effectiveness of paxilline inhibition at both 10 and 100 nM, consistent with the idea that elevation of $[Ca^{2+}]$ diminishes paxilline block. However, when the equilibration condition was changed to −70 mV with 300 µM Ca^{2+} (Po of ~0.07; Fig. 2 C), paxilline inhibition returned to levels more similar to those obtained with 10 µM Ca^{2+} at 0 mV (Fig. 2 A). These results suggest that inhibition by paxilline may not be reduced by increases in Ca^{2+} per se, but by increases in channel Po. Specifically, paxilline inhibition is inversely related to the BK channel Po at the equilibration condition under which paxilline is applied (Fig. 2 D). This inverse relationship between BK Po and inhibition by paxilline immediately excludes the simple case that paxilline exclusively blocks open channels.
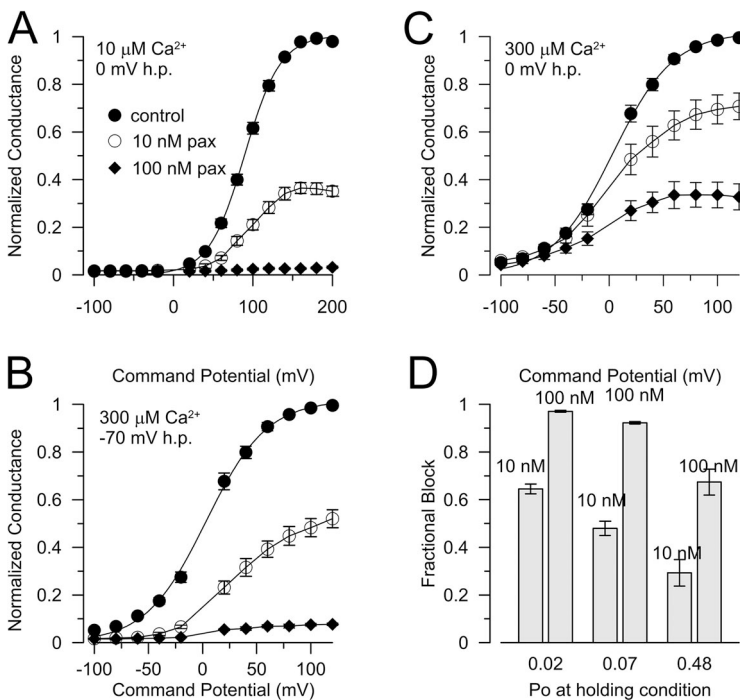
Figure 2. Block by paxilline exhibits an inverse dependence on Po, but no dependence on Ca^{2+} per se. G-V curves were generated under three equilibration conditions (A: 10 µM Ca^{2+}, 0 mV; B: 300 µM Ca^{2+}, 0 mV; C: 300 µM, −70 mV), with either control saline or either of two paxilline concentrations, 10 or 100 nM. For all patches included in this dataset, each patch was examined under all conditions. Paxilline was applied for 4 min before generation of G-V curves. Among different patches, the sequence of holding conditions was varied. G-V curves were normalized to the maximal conductance observed in the absence of paxilline under each holding condition. Curves to control points are fitted single Boltzmann functions, whereas curves in the presence of paxilline have no significance. (D) The fractional block for voltages from 40 to 120 mV was determined for each paxilline application under the three conditions and plotted in relation to the Po at the holding condition defined by the fitted Boltzmann. For 10 µM Ca^{2+} and 0 mV, the effective Po was 0.02; for 300 µM and −70 mV, the Po was 0.07; and for 300 µM Ca^{2+} and 0 mV, the Po at the holding condition was 0.48.

We next examined the inhibition produced by 100 nM paxilline over holding potentials from −80 to 80 mV with constant 300 μM Ca^{2+}, with unblocked current monitored by brief depolarizing steps to 160 mV (Fig. 3 A). Paxilline was washed out between tests at different holding potentials. At holding potentials of −80 and −40 mV, the application of 100 nM paxilline resulted in a similar onset and extent of inhibition (Fig. 3 B). At 0 mV, paxilline inhibition was slower and incomplete, whereas at 80 mV, paxilline produced almost no inhibition over 1 min of application. At the most positive holding potentials in this experiment (40 and 80 mV), the steady-state conductance activated by steps to 160 mV was reduced relative to that at more negative holding potentials. This reflects a very slow inactivation behavior often observed for BK channels activated with strong depolarizations and elevated Ca^{2+} (Fig. 3 C), and does not appear to be related to paxilline inhibition. Overall, this result further supports the view that paxilline block is markedly reduced under conditions favoring open BK channels, whether from elevations in Ca^{2+} or depolarization. Remarkably, paxilline has almost no inhibitory effect under conditions near maximal BK Po.

The weak inhibition by paxilline of BK currents held at positive holding potentials with elevated Ca^{2+} was also tested in a set of patches in which only a single BK channel was expressed. Patches were held either at 70 or −70 mV with 300 μM Ca^{2+}. In one such patch (Fig. 3 D), after the establishment of a given equilibration condition (>45 s), channel activity was monitored first with a 500-msec period at −70 mV and then a 500-msec period at 70 mV, separated by 50 ms at 0 mV (Fig. 3 D, 1). After development of inhibition by 100 nM paxilline at −70 mV, subsequent test steps show essentially no channel activation at either −70 or 70 mV (Fig. 3 D, 2). After return to a holding potential of 70 mV while still in the presence of 100 nM paxilline, channel activity similar to the control behavior was restored at both −70 and 70 mV (Fig. 3 D, 3). Thus, even in the constant presence of paxilline, channels can recover from inhibition at conditions of high Po. After returning the holding potential to −70 mV (while still in the presence of paxilline), complete inhibition was reestablished (Fig. 3 D, 4). Finally, after washout of paxilline while holding at 70 mV, channel activity was restored (Fig. 3 D, 5). Subsequent wash-in of paxilline while holding at 70 mV failed to
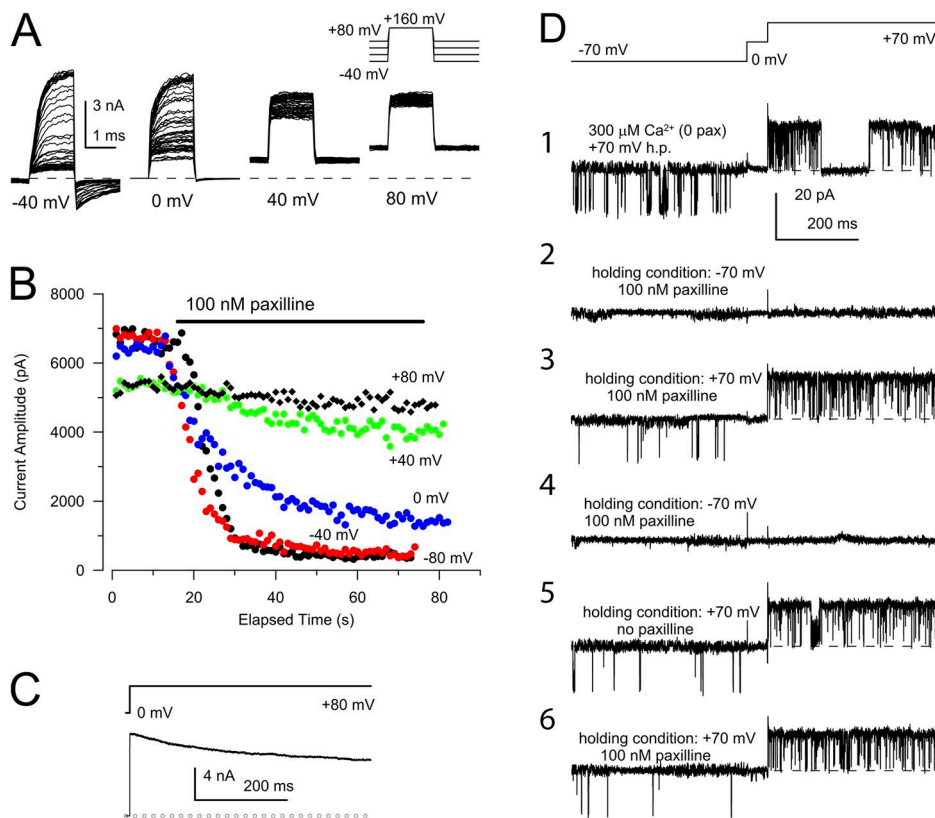
Figure 3. Paxilline inhibits channels at conditions of low Po, but not under conditions of high Po. (A) An inside-out patch bathed with 300 μM Ca^{2+} was initially held at −80 mV. The patch potential was then stepped to holding potentials of −40, 0, 40, and 80 mV (from left to right), and 1.6-ms steps to 160 mV were used to monitor available BK current, while 100 nM paxilline was applied after the 10th step at a given holding potential. Paxilline was washed out and full recovery from block was obtained between tests at different holding potentials. At the most negative potentials, block is substantial, whereas at 40 and 0 mV, there is little development of block. (B) The peak outward current from the traces in A is plotted as a function of elapsed experimental time. (C) The time course of reduction of current during sustained depolarization to 80 mV is shown, establishing that the reduction of current at the positive holding potentials (B) does not reflect paxilline block, but an intrinsic slow reduction in BK conductance with prolonged depolarization. (D) All traces are from the same single-channel patch, stimulated with the protocol shown on the top. The patch was constantly exposed to 300 μM cytosolic Ca^{2+}. (1) Control activity in the absence of paxilline. (2) The holding potential was changed to −70 mV, and 100 nM paxilline was applied. The trace was taken after 30 s in paxilline. (3) The trace was taken ∼30 s after the patch had been returned to 70 mV while in the constant presence of 100 nM paxilline. (4) The trace was taken ∼30 s after the patch was again returned to −70 mV while in paxilline. (5) The trace was obtained after washout of paxilline while holding the patch at 70 mV. (6) The trace was taken ∼30 s after 100 nM paxilline was applied while holding at 70 mV.

restore inhibition (Fig. 3 D, 6). It is noteworthy that during inhibition by paxilline, no openings are observed at all during these brief 500-ms periods at either -70 or 70 mV (Fig. 3 D, 2 and 4). Thus, several 100 ms are not sufficient to allow recovery from paxilline inhibition, even at conditions favoring high Po. However, when the test sequence is applied after equilibration in paxilline at 70 mV, BK openings still occur intermittently during the entire 500 ms at -70 mV (Fig. 3 D, 3). This is generally consistent with the earlier results (Fig. 1 E), indicating that the onset of paxilline inhibition develops over several seconds.

The ability of inhibition by paxilline to be reversed by changes in equilibration conditions, even in the constant presence of paxilline, was also confirmed in patches with large numbers of BK channels (Fig. 4). Specifically, after onset of block in 100 nM paxilline (Fig. 4 A), changing the equilibration conditions to those favoring unblocking can produce recovery from paxilline inhibition (Fig. 4, B and C). It may be noticed that the onset of paxilline inhibition appears variable during wash-in of paxilline. This is addressed below and appears to reflect variability in paxilline access to the patch, despite the rapidity of solution exchange with small charged molecules.

These tests show clearly that inhibition of BK channels by paxilline is reduced or even absent under conditions favoring high Po, whether produced by depolarization or by Ca^{2+}. Qualitatively, the relief of inhibition at high Po suggests either that: (a) if paxilline binds with nanomolar affinity to the open state, it must not occlude permeation; or (b) if paxilline can occlude permeation, it must only bind very weakly to the open state. Most importantly, it suggests that effects on the open state are not central to inhibition by paxilline.

Paxilline inhibits BK NPo under conditions where voltage sensors are largely inactive

Paxilline might favor occupancy of channels in closed states, perhaps without directly occluding the ion permeation pathway, by a variety of mechanisms. In one, the binding of paxilline may alter the C-O equilibrium constant, L, favoring occupancy of closed states. In another, paxilline may stabilize the BK voltage sensors in resting states. A third possibility, that paxilline disrupts the linkage of Ca^{2+} binding to gating, seems unlikely, as increases in Ca^{2+} reduce paxilline inhibition.

At negative potentials where voltage sensors are largely inactive, BK channels open at low Po, even in the absence of Ca^{2+} in accordance with the intrinsic equilibrium (L) between unliganded closed and unliganded open channels (Horrigan and Aldrich, 2002). Under such conditions, increases in cytosolic Ca^{2+} favor additional BK channel activation (Horrigan and Aldrich, 2002). If paxilline is able to reduce NPo when voltage sensors are largely inactive, it would support the possibility

that paxilline alters the C-O equilibrium, in essence reducing the equilibrium constant, L. Patches with a large number of channels were therefore used to obtain estimates of NPo at -80 mV, both at 10 and 300 μM Ca^{2+} (for 300 μM Ca^{2+}, see Fig. 5 A) alone and then with different paxilline concentrations. The NPo in the presence of paxilline was then normalized to the NPo measured for that patch in the absence of paxilline (Fig. 5 B). Paxilline inhibited the BK current by >95% at 100 nM paxilline, both in 10 and 300 μM Ca^{2+}. Because the results above suggest that the effects of paxilline on open states are minimal, the reduction of NPo at negative potentials suggests that paxilline markedly
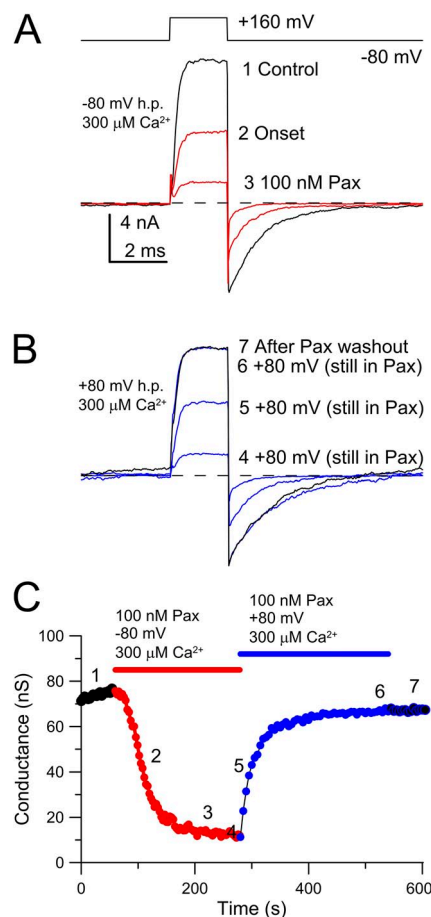
Figure 4. Essentially complete recovery from paxilline block can occur, even in the continuous presence of paxilline under conditions of high Po. (A) The indicated test-pulse sequence was applied every 1 s while holding at -80 mV with 300 μM Ca^{2+}. The traces show before paxilline application, after ~50% inhibition by paxilline, and during the full paxilline effect. (B) For the same patch in A, the equilibration conditions were altered to 80 mV with 300 μM Ca^{2+} while still in the continuous presence of 100 nM paxilline. Brief sojourns to -80 mV with test steps to 160 mV were used to monitor recovery in the presence of paxilline. A 60-s washout of paxilline confirmed that no additional recovery occurred. (C) The time course of onset and recovery from inhibition by 100 nM paxilline, while in the continuous presence of paxilline, is plotted for the cell shown in A and B, with the numbers corresponding to the approximate times of the traces in A and B.

increases the fraction of time a channel is closed. A fit of a simple Hill function (see legend to Fig. 5) to the paxilline-induced reduction in normalized NPo yielded an IC$_{50}$ for inhibition of 5.0 ± 1.5 nM with $n = 0.85 \pm 0.25$, with $n = 1$ clearly better than $n = 2$ (Fig. 5 B). This
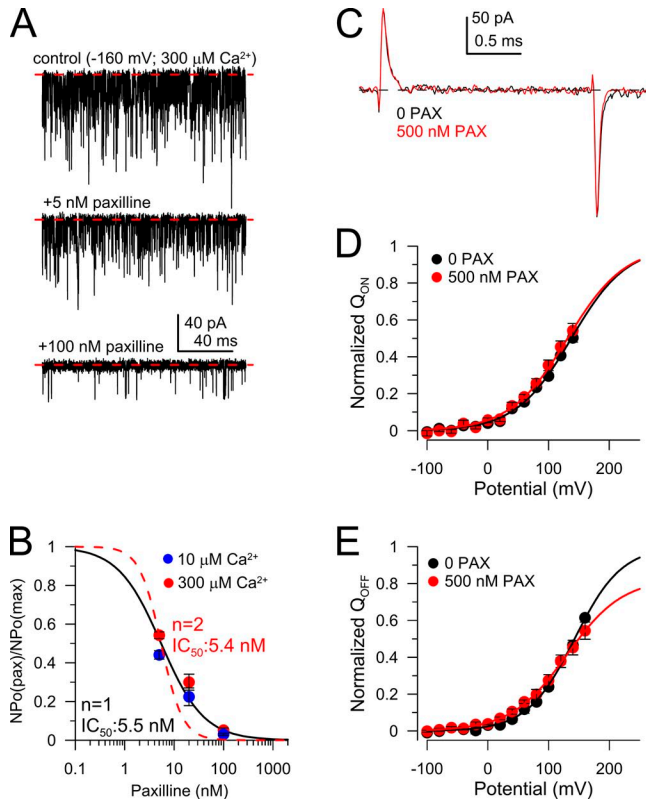
Figure 5. Paxilline reduces NPo at conditions where voltage sensors are largely inactive, and does not influence the voltage-sensor equilibrium. (A; top) The trace shows example channel activity at −80 mV and 300 μM Ca^{2+} for a macropatch with many channels. 4-ms steps to 100 mV (not depicted) were also used to monitor paxilline inhibition. (Middle and bottom) These traces show activity under the same conditions but with 5 and 100 nM paxilline, respectively. NPo was determined from activity at −80 mV. (B) The NPo measured in paxilline for 3 s of activity normalized by the NPo measured in the absence of paxilline is plotted as a function of paxilline. The solid line corresponds to a fit of

$$NPo(pax)/NPo = \frac{1}{1+\left(\dfrac{[PAX]}{IC_{50}}\right)^{n}},$$

with IC$_{50}$ = 5.5 ± 1.1 nM with $n = 1$. Red dotted line corresponds to a fit of the same function with $n = 2$. (C) Gating currents measured with an activation step to 160 mV from −80 mV with 0 μM Ca^{2+} are shown in the absence and presence of 500 nM paxilline. (D) The Q$_{on}$ integrated over 1 ms for steps to the indicated potentials are plotted for control and 500-nM paxilline solutions. Fitted lines correspond to: without paxilline, $z = 0.56 \pm 0.050$ e with V$_{h}$ = 137.6 ± 14.3 mV; with paxilline, $z = 0.54 \pm 0.025$ e with V$_{h}$ = 131.4 ± 2.1 mV. (E) Q$_{off}$ is plotted as a function of previous command potential for 0 and 500 nM paxilline. Without paxilline, $z = 0.66 \pm 0.07$ e with V$_{h}$ = 142.7 ± 14.3 mV; with paxilline, $z = 0.56 \pm 0.035$ e with V$_{h}$ = 130.2 ± 9.1 mV.

result indicates that the binding of paxilline produces a >95% inhibition of BK Po under conditions in which voltage sensors are largely inactive and Po is defined largely by the intrinsic C-O equilibrium.

To evaluate whether the effects of paxilline are independent of any effect on voltage sensors, we measured gating currents in patches containing large numbers of channels, both in the absence and then in the presence of 500 nM paxilline (Fig. 5 C). The gating current associated with activation steps (Q$_{on}$) was determined over a range of activation voltages and normalized to the fitted Qon$_{(max)}$ defined from a simple Boltzmann (Fig. 5 D). The Q$_{on}$ versus command potential relationship was essentially identical in the absence and presence of 500 nM paxilline. Q$_{off}$ was also determined in the presence and absence of paxilline (Fig. 5 E). Although any effect of paxilline on Q$_{off}$ is small, the duration of the activation step preceding the off-step is likely to have been sufficient to have caused some channels to open in the absence of paxilline, while less likely to have opened in the presence of paxilline. Thus, the Q$_{off}$ relationship in paxilline likely reflects solely equilibration of voltage sensors among closed states, whereas in the absence of paxilline, there may be contributions of voltage sensors, as some channels pass from open to closed states. Regardless of the origins of the slight difference observed in Q$_{off}$, the results provide strong support for the idea that paxilline does not alter the voltage-sensor equilibrium nor impede voltage-sensor movement.

Inhibition of BK current is best explained by binding to and stabilization of closed states

100 nM paxilline reduced the normalized NPo to <0.05 at −80 mV and 300 μM Ca^{2+}. This is consistent with a mechanism in which binding of paxilline reduces the intrinsic O/C ratio by >0.05, favoring occupancy of closed channels. However, the data do not distinguish among different models of block involving closed-channel stabilization. The recognition that unblock from paxilline can be facilitated by high Po conditions prompted us to pursue a more extensive examination of the paxilline concentration dependence under different equilibration conditions. We therefore examined the concentration dependence of paxilline inhibition over a range of equilibration conditions that span a wide range of BK Po. Specifically, paxilline inhibition was examined with equilibration conditions of 300 μM Ca^{2+} at −70 mV (Fig. 6, A and C), 0 mV, 40 mV (Fig. 6, B and D), and 70 mV. For the set of patches used in this experiment, these equilibration conditions corresponded to effective Po's of ∼0.1, ∼0.65, ∼0.83, and ∼0.89. For each equilibration condition, fractional inhibition was determined for at least four different paxilline concentrations (Fig. 6, A–D). To monitor block under each of these conditions, brief 2-ms test steps to

160 were used, which do not alter the fraction of channels blocked by paxilline. Current activated by the brief test steps corresponds to that fraction of channels in all unblocked states at the equilibration conditions. For paxilline application under conditions of highest Po (either 40 or 80 mV at 300 µM Ca^{2+}), the slow onset of inhibition posed challenges to a direct determination of steady-state inhibition. In such cases, a fit of a single exponential to the onset of block (Fig. 6 D) was used to obtain an extrapolated estimate of fractional inhibition. Furthermore, despite the ability of high Po to reduce inhibition by paxilline, at the highest paxilline concentrations full wash-out was difficult to achieve, perhaps because of accumulation of paxilline within the recording pipette during the long durations of

paxilline application. To minimize uncertainties arising from cumulative inhibition, at the highest Po condition patches were only used for one to two paxilline applications (e.g., Fig. 6, B and D). Consistent with earlier experiments, the concentrations of paxilline required to produce inhibition at conditions of high Po were orders of magnitude higher than those required at lowest Po.

From this type of experiment, the fractional inhibition by paxilline shifts markedly rightward as the equilibration conditions result in channels of higher Po (Fig. 6 E). If one fits a simple Hill equation through the plot of fractional unblock as a function of [paxilline] under each equilibration condition (Fig. 6 E, red dotted lines), the apparent IC_{50} for paxilline inhibition
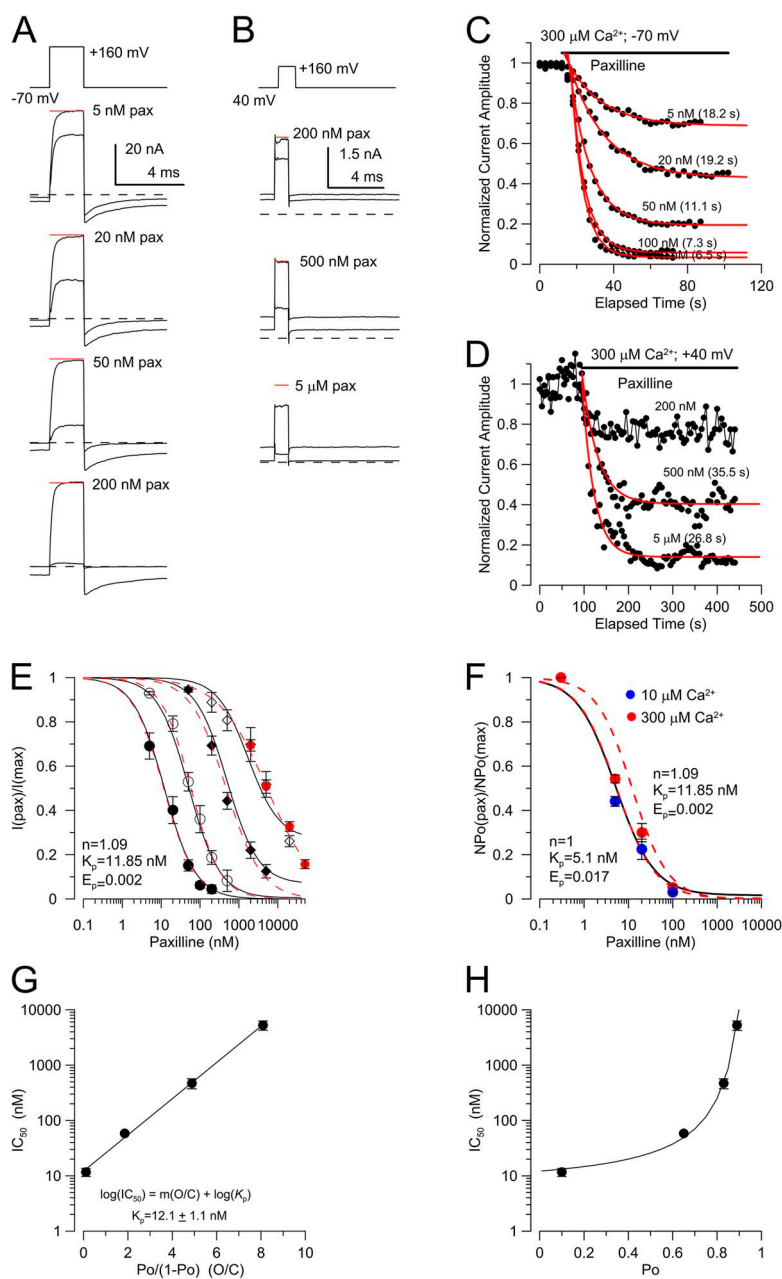
Figure 6. Concentration dependence of paxilline inhibition at four different conditions of channel Po. (A) Traces show currents activated by brief steps to 160 mV under equilibration conditions of −70 mV and 300 µM Ca^{2+} with 5, 20, 50, and 200 nM paxilline. Red line shows the identical level of peak current for each paxilline test. (B) Traces show currents activated by steps to 160 mV under equilibration conditions of 40 mV and 300 µM Ca^{2+} for 200 nM, 500 nM, and 5 µM paxilline, all from the same patch. (C) The onset of inhibition of current activated at 160 mV with 300 µM Ca^{2+} at −70-mV equilibration condition from traces as in A is shown for five paxilline concentrations along with single-exponential fits (red). (D) Onset of inhibition with single-exponential fits (red) is shown for the higher Po equilibrium condition (B). (E) The fraction of unblocked BK current is plotted as a function of paxilline for four different equilibration conditions (−70, 0, 40, and 70 mV, all with 300 µM Ca^{2+}) from experiments as in A and B. Dotted red lines correspond to fits of a Hill function, with IC_{50} values of 11.7 ± 1.9 nM, 58.4 ± 2.9 nM, 469.8 ± 94.9 nM, and 5.37 ± 1.0 µM, from left to right. Solid lines correspond to the fit of Scheme 1, with K_p = 11.85 nM and E_p = 0.002, with n = 1.09. (F) The inhibition of NPo at −80 mV and either 10 or 300 µM Ca^{2+} is displayed from Fig. 5 B, with the dotted red line corresponding to the best fit from Scheme 1 (E) (K_p = 11.85 nM). (G) IC_{50}s from E are plotted as a function of O/C and fit with $\log(IC_{50})$ = $m(O/C) + \log(K_{cp})$, where m (0.33 ± 0.02) is the slope of the relationship and K_p (12.1 ± 1.1 nM) is the extrapolated IC_{50} with all channels closed. This provides a model-independent estimate of paxilline inhibition of closed channels. (H) IC_{50} estimates are replotted as a function of Po along with the fit in F. The extrapolation of the line to Po of ∼1 provides a model-independent estimate of paxilline inhibition of open channels.

shifts from 11.7 nM, 58.4 nM, 469.8 nM, to 5.3 µM over the equilibration conditions of −70, 0, 40, and 70 mV all at 300 µM Ca^{2+}. This provides additional strong support for the unusual state dependence of paxilline inhibition, with inhibition being much more strongly favored under conditions of low Po. If we assume that the effect of paxilline arises solely from an alteration in the C-O equilibrium constant, L(0) as defined in Scheme 1, a fit of this model (Eq. 1) yields K_p = 11.9 ± 2.3 nM, with n = 1.09 ± 0.11 and E_p of ∼0.002 (Fig. 6 E, black lines). This dataset and model imply that the binding of paxilline to the open channel is ∼500-fold weaker than the binding to closed channels, and that a single

paxilline molecule produces the inhibitory effect. This model also assumes that the binding of paxilline to the open state does not block conductance. An interesting feature of this model is the tendency toward flattening of the predicted block curves at <100% block at the highest paxilline concentrations. Although this estimate of K_p is somewhat greater than estimated in the measurements of paxilline inhibition under conditions of inactive voltage sensors (Fig. 5, A–C), the fitted value of Scheme 1 for the low Po situation provides a satisfactory approximation of the reductions of NPo (Fig. 6 F). The suitability of this model and other models will be addressed in more detail below.
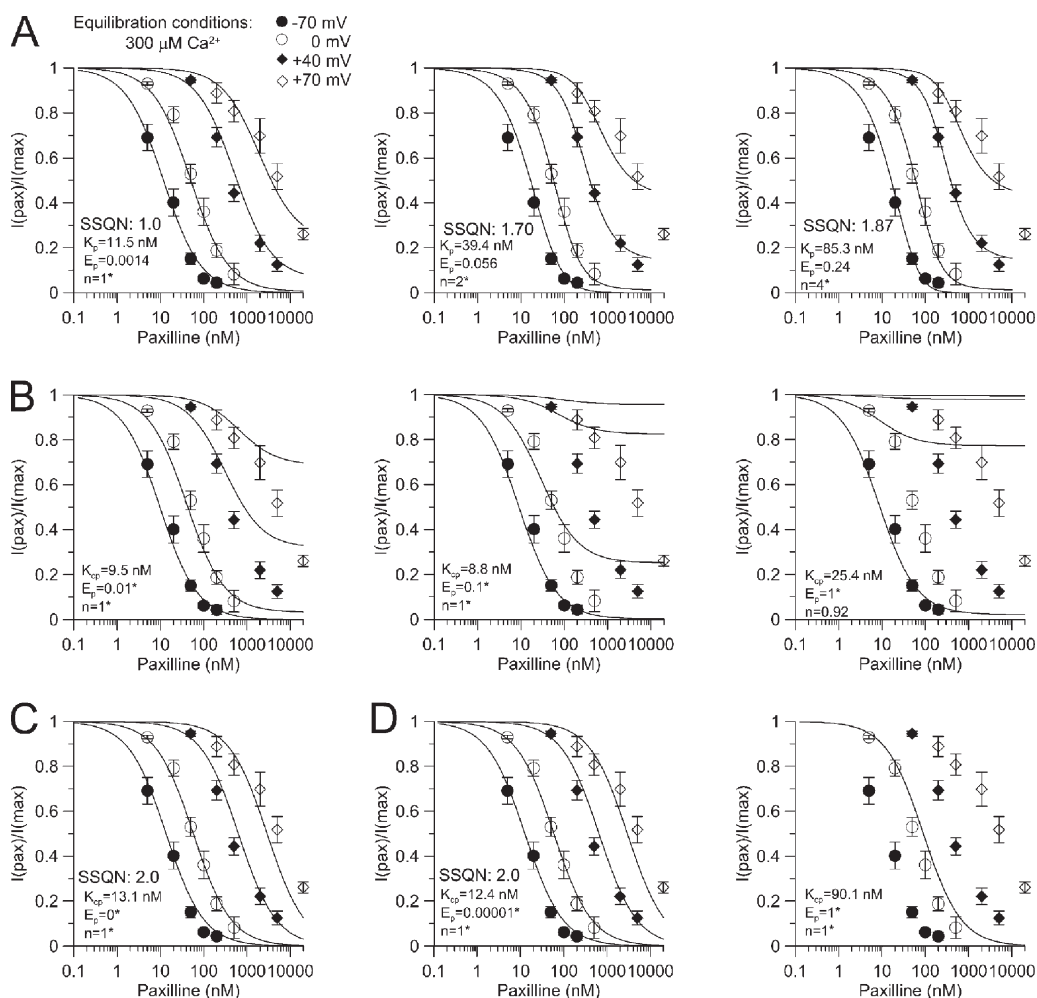
Figure 7. Paxilline stabilizes closed states with only weak, if any, binding to open states. (A) Curves of concentration-dependent inhibition of BK current at four equilibration conditions were fit with Scheme 1, with the assumption that the current activated at positive potentials reflects channels initially either in C, O, or OB, i.e., any open channels with bound paxilline are conducting. Each panel from left to right corresponds to fits with Scheme 1 (Eq. 7) in which either one, two, or four paxilline molecules can bind to inhibitory positions. Best-fit values are given in the figure. The model with n = 1 best accounts for the shape of the inhibition by paxilline. (B; left) Scheme 1 was again used, while constraining E_p to 0.01 (left), 0.1 (middle), or 1.0 (right), showing that increasing open-state affinity fails to account for the data. Right-hand panel corresponds to state-independent paxilline interaction with C and O. (C) E_p was set to 0, thereby approximating strictly closed-channel block. (D) Data were fit with Scheme 3 (Eq. 3) in which the paxilline-bound open state is nonconducting. On the left, the value for E_p drifted toward 0, similar to a strictly closed-channel block situation. On the right, E_p was set to 1 (state-independent binding of paxilline). SSQN in A and C corresponds to the sum-of-squares for a given fit normalized to the sum-of-squares for the left panel in A.

Another way of viewing the inhibition by paxilline is to plot the nominal IC_{50} (estimated from the fit of $NPo(pax)/NPo(max) = 1/(1 + [PAX]/IC_{50})$ relative to state occupancy. Specifically, a plot of IC_{50} versus $Po/(1 - Po)$ (Fig. 6 G) provides some largely model-independent conclusions about paxilline action. Empirically, $\log(IC_{50})$ varies linearly with $Po/(1 - Po)$ over a broad range of closed-state occupancies. At the limit of maximal C-state occupancy, for this set of data the limiting IC_{50} is 12.1 ± 1.1 nM, which essentially provides a model-independent estimate of the closed-state affinity for paxilline (Fig. 6 G). As C-state occupancy decreases, IC_{50} changes almost 1,000-fold, implying that if paxilline binds to and inhibits open states, it must do so at an affinity almost 1,000-fold weaker than binding to the closed states. The lack of horizontal asymptote in the relationship between IC_{50} as a function of Po (Fig. 6 H) also strongly suggests that the open state is not directly inhibited at concentrations up to 10 µM.

Allosteric regulation of the C-O equilibrium constant, L, best explains paxilline action

Although Scheme 1 yielded a very satisfactory fit of the reduction of current as a function of paxilline, we next assessed whether other variations of Scheme 1 or other schemes that include closed-channel block would also be consistent with the data. First, we compared the extent to which the quality of the fit with Scheme 1 was dependent on whether one, two, or four paxilline molecules could all occupy inhibitory positions. Eq. 1 was modified (Eq. 7) to reflect up to n paxilline-binding sites, where each site independently influences the C-O equilibrium. This is analogous to the regulation of L by Ca^{2+} (Horrigan and Aldrich, 2002), except that instead of increasing BK activation, activation is inhibited.

$$f_{un}(Pax, hp) = \frac{\overline{L_{hp}} + \left(1 + \dfrac{E_p[Pax]}{K_p}\right)^n}{\left(1 + \dfrac{E_p[Pax]}{K_p}\right)^n + \overline{L_{hp}}\left(1 + \dfrac{[Pax]}{K_p}\right)^n}. \quad (7)$$

When paxilline inhibition is assumed to involve two or four independent sites, the resulting fits do a less adequate job of approximating the data compared with a single paxilline-binding site (Fig. 7 A). This therefore suggests that, wherever the site of paxilline action within the BK tetramer, a channel can probably only accommodate a single paxilline molecule.

Both the model-independent analysis in Fig. 6 and the fit of Scheme 1 to the concentration dependence of paxilline inhibition (Fig. 7 A) indicate a nearly 1,000-fold difference between paxilline affinity between closed and open states. We next compared the consequence of assuming a smaller difference in affinity ($E_p = 0.01$, 0.1, or 1) in Scheme 1 (Fig. 7 B). Even with a 100-fold difference

in closed- and open-state affinity ($E_p = 0.01$), the resulting fit is completely inadequate, again supporting the view that paxilline exerts a very strong effect on the C-O equilibrium. The case in which $E_p = 1$ (Fig. 7 B, right) corresponds to a completely state-independent form of Scheme 1. In this case, inhibition is absent for the higher Po conditions, even at maximal [paxilline], as both O and O_p are conducting states.

Do the results permit us to exclude other models? The value of E_p estimated from the fit of Scheme 1 immediately suggests that the dataset is unlikely to strongly distinguish among the different models. To evaluate this directly, we first fit the paxilline concentration dependence of inhibition with Scheme 2 (Fig. 7 C; closed-state inhibition alone; Eq. 2). This results in an adequate fit of the data, although not as good as with Scheme 1. With Scheme 3 (both closed and open states can be inhibited by paxilline; Eq. 3), convergence was only achieved when E_p was set to very small values, essentially making it identical to closed-channel block (Fig. 7 D). A state-independent form ($E_p = 1$) of Scheme 3 illustrates that, under all conditions of Po, inhibition by paxilline would be identical.

These results strongly support the idea that the binding of a paxilline molecule to a BK channel strongly stabilizes closed states, corresponding to a >500-fold reduction in the C-O equilibrium constant, $L(0)$. Furthermore, the analysis suggests that only one paxilline molecule can act on a BK channel at a time. Can we exclude the possibility that paxilline does not bind to open channels at all? Thermodynamically, that is unlikely. Although the optimal fit was achieved for Scheme 1, the differences among Fig. 7 A (left), Fig. 7 C, and Fig. 7 D arise largely from the data points at 300 µM Ca^{2+}, 70 mV, at the highest paxilline concentrations. Both Schemes 2 and 3 predict stronger block and essentially complete block at the highest concentrations, whereas Scheme 1 predicts some finite current at the highest paxilline concentrations, as open paxilline-bound channels are conducting. Unfortunately, it is the estimates of fractional inhibition at 5 and 20 µM paxilline that are the most technically challenging and probably most subject to errors, as fractional block was often estimated from extrapolation of a fitted exponential. Yet, despite this uncertainty, the key point is that paxilline affinity between closed and open states differs markedly. In fact, for all practical purposes, for conditions under which paxilline is typically used to inhibit BK channels, only closed-channel binding and stabilization are relevant.

Kinetics of onset of paxilline inhibition

An examination of the kinetics of the onset and recovery from paxilline inhibition and dependence on paxilline concentration may help provide additional insight into mechanism. However, as noted in regards to Fig. 1 E,

we observed that, despite identical conditions of Po, stimulation, and paxilline concentrations (compare Figs. 1, G–H, 3 B, 4 C, and 8 A), the apparent onset of inhibition, when paxilline is washed onto a patch, appeared to vary substantially from patch to patch. However, with the realization that the paxilline-blocking equilibrium can be simply shifted from blocked to unblocked by changes in patch equilibrium conditions, we wondered whether consistent estimates of block onset and recovery could be obtained by shifts in the equilibration conditions while maintaining patches in the continuous presence of paxilline.

As a first step, we compared the apparent onset of paxilline inhibition both from direct wash-in of paxilline
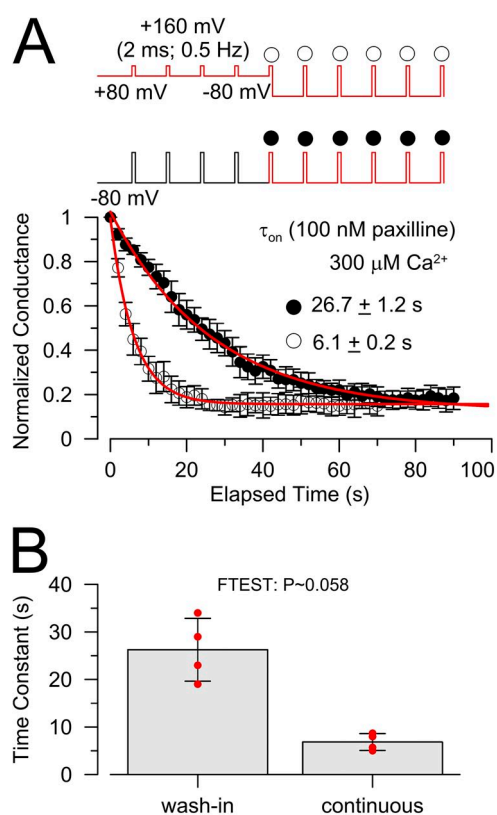
Figure 8. Kinetics of block onset is more reliably estimated by step changes in equilibration conditions while in the constant presence of paxilline rather than by wash-in of paxilline. (A) Onset of paxilline is compared at -80 mV and 300 µM Ca^{2+} for two situations: first, simple perfusion of 100 nM paxilline over the cytosolic face of the face, and second, a change in equilibration conditions from 80 to -80 mV. Voltage protocols in each case are shown schematically. Available BK current was monitored by a 2-ms step to 160 mV applied at 0.5 Hz. Symbols over the voltage steps for a particular protocol correspond to the particular symbols showing the onset of block as a function of elapsed time, with single-exponential time constants as given. (B) Estimates of time constants from individual patches for each method of assessing paxilline block are shown along with means and STD. Each method was evaluated with the same patches. An F-test provided an assessment of whether variance for each set of estimates was significantly different.

and also from changes in equilibration conditions in the same set of patches (Fig. 8). For this set of four patches, the onset of inhibition by simple wash-in of 100 nM paxilline at -80 mV with 300 µM Ca^{2+} occurred with a time constant of τ_{on} of 26.3 ± 6.6 s (mean ± STD). In contrast, after establishing a steady-state unblocked (Fig. 8 A; 80 mV; 100 nM paxilline) condition, the holding potential was changed to promote block (Fig. 8 A; -80 mV). In this case, the onset of paxilline inhibition (-80 mV, 300 µM Ca^{2+}) developed with a time constant of 6.85 ± 1.79 s, about fourfold faster than that observed with paxilline wash-in (Fig. 8 A). The variance of estimates obtained from paxilline wash-in was significantly greater (F-test) than that from estimates derived from changes in equilibration conditions. Although our solution-exchange system generally allows for complete exchange of readily soluble molecules within a few hundred milliseconds (e.g., Fig. 14 A), we suspect that the slow onset of paxilline inhibition during wash-in may be influenced by a slow increase in paxilline concentration within the omega of the inside-out patch, given the tendency of paxilline to stick to or partition into any available hydrophobic surface–including membranes.

The variability and slower onset of inhibition that occurs with direct paxilline perfusion suggests that wash-in is not a useful method for assessing kinetic aspects of paxilline inhibition. However, the kinetics of block onset, while in the continuous presence of paxilline, is likely to represent some intrinsic kinetic step in the paxilline inhibitory equilibrium. We therefore measured the onset of paxilline inhibition under a more extensive set of conditions. First, after equilibration with 100 nM paxilline at 80 mV and 300 µM Ca^{2+}, during which no inhibition was observed, we then examined the onset of paxilline inhibition at potentials from 20 mV to -60 mV (Fig. 9, A and B), using a protocol identical to that used in Fig. 8 A. The rate of inhibition varied over ~20-fold from 20 to -60 mV (Fig. 9, B and D). The onset of inhibition was reasonably well fit with a single-exponential function, but at some conditions of intermediate closed probability (Pc), a double-exponential function yielded a clearly superior fit (Fig. 9 C), with the resulting sum-of-squares improved four- to fivefold. The rate of block was plotted as a function of Pc, the probability of being closed, using the mean rate from fits of the single exponential using the faster rate when a two exponential better described the time course. The rate of inhibition is clearly faster when channels are primarily closed (Fig. 9 D). However, using exclusively the rate obtained from the single-exponential fit, the relationship exhibits a superlinearity that does not follow immediately from the idea that the rate of block depends exclusively on Pc. For a simple two-state gating scheme where opening and closing rates are at rapid equilibrium compared with the microscopic block rate, the observed rate of block might be expected to scale linearly with Pc as
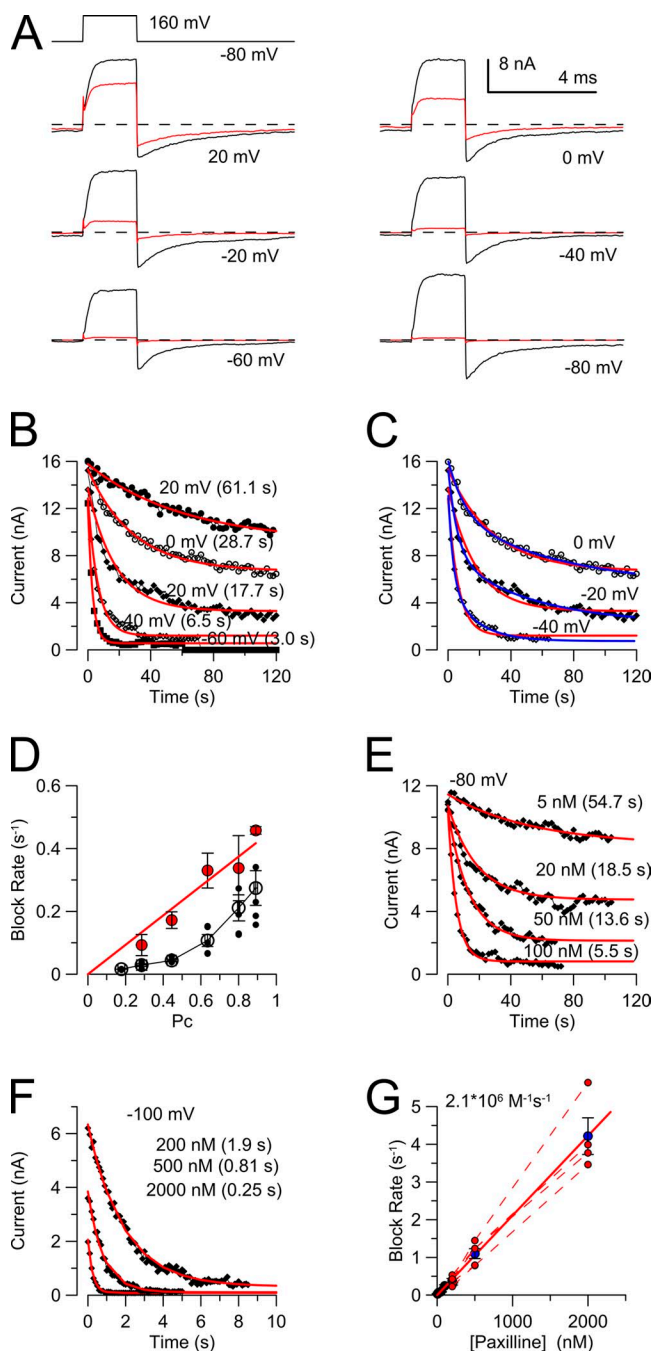
Figure 9. Paxilline inhibition is faster at higher closed-channel probabilities. (A) All traces were obtained from the same patch with the indicated voltage protocol while in the continuous presence of 100 nM paxilline and 300 µM Ca^{2+}. Black traces correspond to currents activated after a re-equilibration period at 80 mV (with 300 µM Ca^{2+}), whereas red traces are the final trace after a change to a new equilibration voltage (as indicated). (B) The onset of current inhibition from the examples in A is plotted as a function of time at the new equilibration potentials. Red lines are single-exponential fits to the onset of inhibition. (C) Onset of inhibition at intermediate Pc is better fit with two (blue) exponential components than one (red). (D) The rate of block (means, SEMs, and individual estimates) from experiments as in B is plotted as a function of Pc, with Pc calculated from the G-V curves at 300 µM Ca^{2+}. Closed red symbols correspond to the

$k_c/(k_c + k_o)$. However, when the faster component of the inhibition onset is used for the intermediate Pc conditions, the overall relationship between the fast onset of block and Pc is linear, with asymptote at 0, consistent with the idea that the initial step in block onset depends on Pc. One potential explanation for the two exponential components is that, at the intermediate and low Pc values, there are additional transitions, either from the gating equilibrium or the blocking mechanism, which contribute to the observed block onset. However, at present, we have no simple explanation for the basis for the two relaxation components at the intermediate Pc values. Regardless of this uncertainty, the results are compatible with the idea that fast components of inhibition vary linearly with occupancy of channels in closed states.

Next, we examined the concentration dependence of the onset of inhibition by paxilline at −80 and −100 mV (Fig. 9, E and F). For estimates at the highest paxilline concentrations, the time between test steps to monitor BK activation was reduced to 0.2 s (Fig. 9 F). Remarkably, over the range of 5 to 2,000 nM paxilline, the rate of block was linear, with a slope of $2.1 \times 10^6 \, \mathrm{M^{-1}s^{-1}}$ (Fig. 9 G). Because these rates are measured under conditions in which the BK channels are primarily closed, this potentially defines the rate of inhibition of a closed channel. This pseudo–first-order molecular association rate for paxilline interaction with a closed channel is remarkably similar to that of uncharged anesthetics acting upon nicotinic AChRs (Adams, 1976) and also the 0-voltage forward rate of inhibition of quaternary ammonium blockers of ligand-gated channels (Neher and Steinbach, 1978; Lingle, 1989).

Collectively, these tests of the rate of onset of inhibition by paxilline support the idea that inhibition involves specific interaction with closed-channel conformations.

The paxilline unblocking rate is only mildly dependent on conditions that favor increased Po

The rate of unblock from paxilline may also be informative regarding the blocking mechanism. In particular, blocking Schemes 1 and 2 make very different predictions for what might be expected during a change in equilibration conditions. In Scheme 1, closed channels stabilized by paxilline have two potential pathways for recovery from inhibition, one being simple unbinding of paxilline from the closed channel, and the other being unbinding after the channel has first undergone

---

faster rate resulting from the fit of either one or two exponential components to the onset time course in B and C. (E and F) Onset of inhibition at −80 mV (E) and −100 mV (F) is shown for different paxilline concentrations along with single-exponential fits. (G) Blocking rate is plotted as a function of [paxilline]. The fitted red line has a slope of $2.1 \times 10^6 \, \mathrm{M^{-1}s^{-1}}$. Each dotted line connects determinations at different [paxilline] for single patches.

a closed to open conformational change. For Scheme 2, unblock can only occur from the closed state. Therefore, Scheme 1 predicts that unblock may be favored by conditions that increase Po, whereas Scheme 2 predicts that the rates of recovery will only depend on dissociation of paxilline from closed conformations. However, in accordance with Scheme 1, given that paxilline has a strong effect on the C-O equilibrium, i.e., E_p of ~0.002, the C to O transition for paxilline-bound channels may still be sufficiently small so that unblock only arises from paxilline unblock from closed channels.

To examine unblocking kinetics, we first allowed block in 100 nM paxilline to develop at −80 mV with 300 µM Ca^{2+}. We then examined unblock from paxilline either after a change to an equilibration condition of higher Po in the constant presence of paxilline or after washout of paxilline. Recovery of channels from paxilline inhibition was assessed by brief test steps to

160 mV, which by itself produces no effect on paxilline recovery. The time course of recovery was essentially identical for either recovery procedure, i.e., a change in equilibration condition (black symbols in Fig. 10 A) or washout of paxilline (red symbols in Fig. 10 A). The time constant of recovery was about twofold briefer at 80 mV compared with 0 mV. At more negative voltages corresponding to conditions of lower Po, the fractional unblock resulting from a change in equilibration conditions precluded careful delineation of the recovery time course. However, the correspondence of the time constants measured either from washout or the change in equilibration allowed simple washout of paxilline to be used to define unblock at conditions of lower Po (Fig. 10 B). For another patch, after the development of inhibition by three separate applications of 100 nM paxilline at −80 mV with 300 µM Ca^{2+}, recovery from inhibition was monitored at −80, −40, and 0 mV (Fig. 10 B),
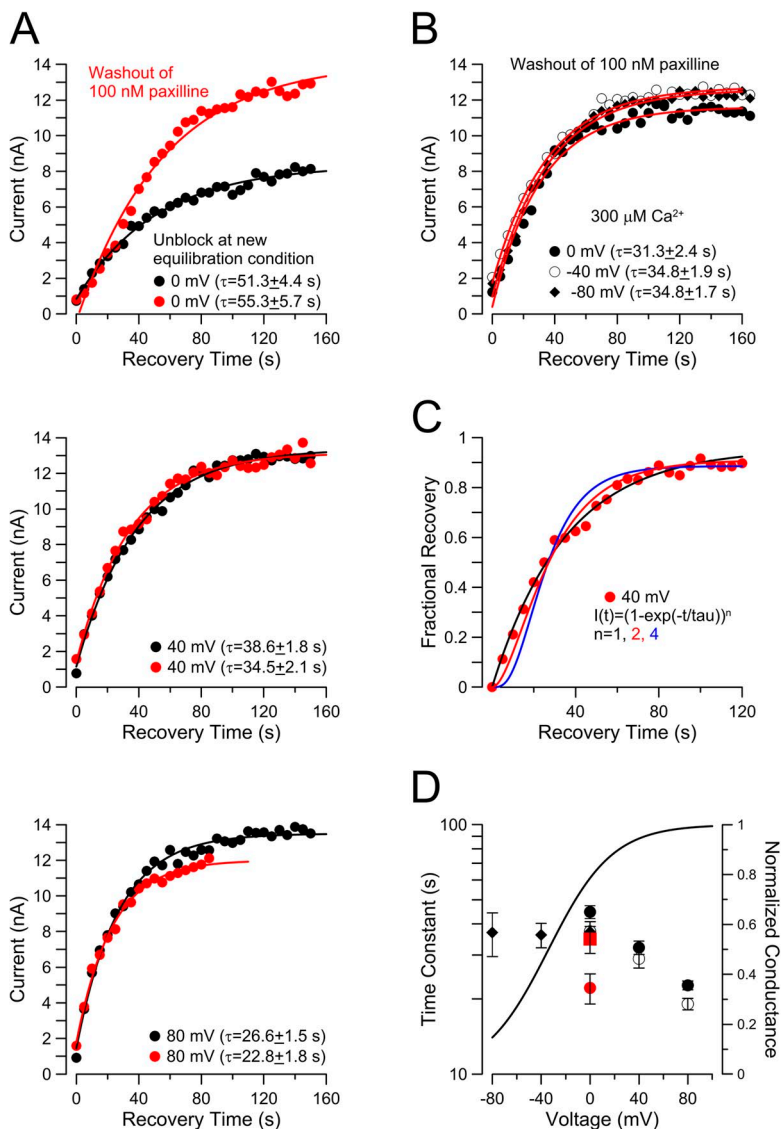
Figure 10. Recovery from paxilline inhibition is faster at higher Po. (A) Unblock time constant from washout of paxilline is comparable to unblock during change in equilibration conditions. The panels are all from the same patch, with the unblocking time course examined at 0 (top), 40 (middle), or 80 mV (bottom). Black symbols and fitted line correspond to unblock in the constant presence of 100 nM paxilline after a change in equilibration condition from −80 mV, 300 µM Ca^{2+} to each of the three voltages. Red symbols and fitted red lines correspond to washout of paxilline at the indicated voltage with 300 µM Ca^{2+}. BK availability was assessed with brief test steps to 160 mV. Po during the recovery conditions was estimated from G-V curves as 0.7 (0 mV, top), ~0.85 (40 mV, middle), and ~0.9 (80 mV, bottom). (B) Recovery time course was compared in the same patch for washout of paxilline at 0 (Po of ~0.7), −40 (Po of ~0.4), and −80 mV (Po of ~0.1), all in 300 µM Ca^{2+}. (C) Recovery time course from A (middle) for washout of paxilline is plotted on a logarithmic scale along with fits of an exponential of form $I(t) = (1 - \exp(-t/tau))^n$, for $n = 1$, 2, or 4. (D) Open circles show recovery time constants for patches examined as in A, with closed symbols corresponding to time constants measured during paxilline washout, and open circles corresponding to the constant presence of paxilline, with each point reflecting the mean of at least four patches. Closed diamonds correspond to time constants measured as in B. The fitted G-V curve ($V_h = -34.0$ mV; $z = 0.98$) for currents activated in the patches in A and B is shown to highlight the extent of changes in fractional activation for the different recovery conditions. Red symbols correspond to seven patches for which recovery was measured at 0 mV in the constant presence of either 100 nM paxilline (red square) or 20 nM paxilline (red circle).

revealing essentially no difference in recovery time course among these three conditions.

Analysis of recovery time course can also be useful in distinguishing among different types of inhibitory mechanisms. The single-exponential nature of the recovery time course is consistent with a single rate-limiting step, perhaps paxilline unbinding, underlying the recovery as embodied in Scheme 1. A different category of model not considered in the analysis of steady-state inhibition would involve multiple, identically bound paxilline molecules, each of which must dissociate before unblock occurs. In such a case, the time course of recovery is expected to exhibit a lag, consistent with the number of recovery steps. However, we found that the recovery time course, when defined by $I(t) = (1 - \exp(-t/\text{tau}))^n$, consistently yields values near 1 (Fig. 10 C), whereas constraining $n = 2$ or 4 totally fails to describe the recovery time course. Thus, there is no indication of any delay in the onset of a single-exponential unblocking process.

Mean values from similar recovery experiments revealed little obvious difference in unblocking time constants from −80 to 0 mV, with only a modestly faster time constant at more positive voltages (Fig. 10 D). It is noteworthy that, after a change in the voltage to allow unblock to occur, the recovery time course is essentially identical whether paxilline remains in the solution or is washed out. However, in another set of seven patches, we explicitly measured recovery at 0 mV in the constant presence of paxilline, with paxilline either at 20 or 100 nM (red symbols in Fig. 10 D). In this case, the fivefold

difference in paxilline concentration was associated with a 1.6-fold different in recovery time constant. This weak concentration dependence seems curious given the similarity of recovery from inhibition by 100 nM paxilline, when recovery occurs either with or without paxilline. We potentially attribute this difference to the idea that channels recovering at 0 mV from inhibition by 20 nM paxilline begin with only slightly more blocked channels than unblocked channels, whereas channels recovering with 100 nM paxilline start primarily from blocked states. We noted above that the time course of inhibition onset at intermediate Po levels exhibits some complexity, perhaps reflecting the contributions of multiple transitions to the observed relaxations. We suggest that the same may apply when comparing unblock at 20 nM paxilline to that at 100 nM paxilline.

Collectively, these tests show that conditions of increased Po only weakly increase the rate of recovery from paxilline inhibition and only at the most positive Po's. The absence of any obvious effect of conditions favoring channel opening on unblock at potentials negative to 0 mV suggests that, under such conditions, inhibition by paxilline is defined solely by the rates of association to and dissociation from the closed channels. Excluding the possibility that paxilline binding is directly influenced by voltage and/or Ca^{2+}, we favor the view that the weak Po dependence of unblock rate at positive voltages is consistent with Scheme 1; that is, some closed channels bound with paxilline recover by first opening, which then permits faster dissociation of
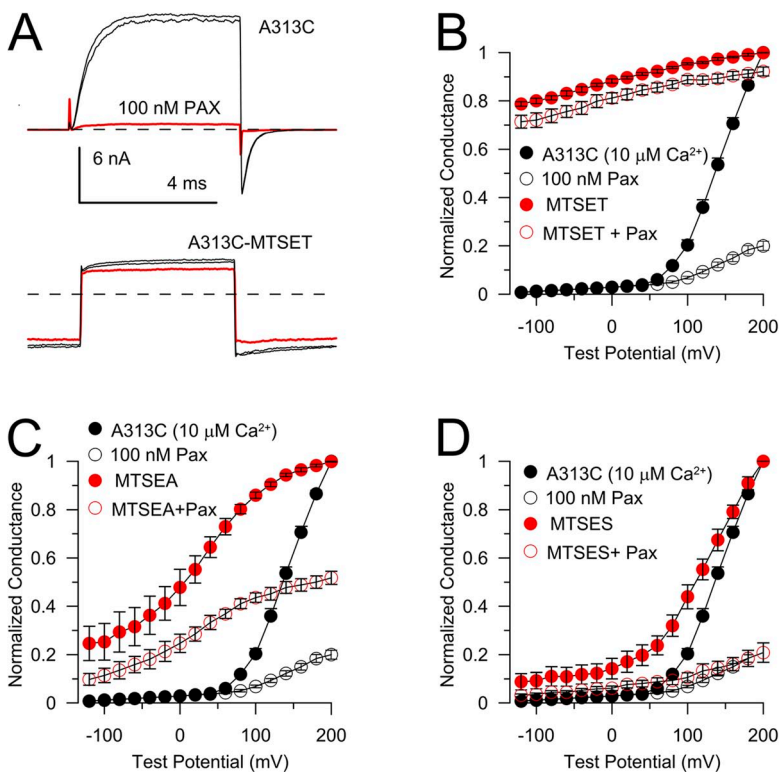
Figure 11. Manipulation of BK Po by MTS modification of S6 residues also modulates paxilline sensitivity. (A) Traces on the top show that 100 nM paxilline readily blocks Slo1-A313C currents, but after modification of A313C with MTSET, paxilline produces hardly any block of the residual current. (B) The normalized conductances from the experiment shown in A are plotted for A313C in the absence and presence of paxilline, and then after modification by MTSET. Slo1-A313C-MTSET is constitutively active over the potentials examined. (C) Results are shown for Slo1-A313C before and after modification by MTSEA. Modification by MTSEA produces less G-V shift than for modification by MTSET, whereas block by paxilline is also intermediate. (D) Similar results are shown for Slo1-A313C before and after modification by MTSES. MTSES produces only modest shifts in the BK G-V and has little effect on block by paxilline.

paxilline, reflecting the very weak affinity of paxilline to the open channel. That unblocking rates are not more strongly Po dependent suggests that paxilline unbinding from closed states is still relatively rapid compared with opening of the paxilline-closed state, even at positive voltages and high Ca^{2+}.

The above interpretation suggests that the time constants of recovery measured at negative voltages reflect the dissociation rate of paxilline from closed channels. The mean time constant at -80 mV of 37.0 s corresponds to a rate of 0.027/s. From the forward rate of paxilline block to closed channels of 2.1×10^6 $M^{-1}s^{-1}$ (Fig. 9 F), the affinity of paxilline to the closed BK channel calculated from the kinetic estimates is 12.9 nM, in quite satisfactory agreement with the estimates of paxilline affinity for the closed channel based on inhibition of steady-state currents (Fig. 6 E).

Pore modification with MTS reagents alters paxilline inhibition in a fashion consistent with the inverse dependence of inhibition on Po

MTS modification of a cysteine introduced at A313 in the BK S6 helix shifts BK G-V curves to more negative potentials (Zhou et al., 2011). The extent of the gating shift depends on the MTS reagent, with MTSET resulting in the largest shifts. We therefore wondered whether gating shifts produced by the MTS reagents might alter paxilline sensitivity in a fashion consistent with the Po dependence of paxilline block. We first defined the paxilline sensitivity of the unmodified A313C construct (Fig. 11, A and B). 100 nM paxilline resulted in strong block of the Slo1-A313C current. The application of 100 µM MTSET resulted in an irreversible modification of the Slo1-A313C current with strong current rectification at positive potentials, reflecting a voltage-dependent reduction of single-channel conductance by the MTSET attached to A313C (Zhou et al., 2011). Furthermore, modification by MTSET produces an essentially constitutive activation of current at negative potentials (Fig. 11 A), as indicated by G-V curves generated from the Slo1-A313C-MTSET tail currents (Fig. 11 B). The application of 100 nM paxilline to the MTSET-modified channel produced only a small reduction in current (Fig. 11 A). The Po of the MTSET-modified Slo1-A313C channels was ~0.9 at 0 mV with 10 µM Ca^{2+}, whereas the fractional block by paxilline was <0.1.

The disruption of paxilline inhibition of the MTSET-modified channel might arise either from the inability of paxilline to inhibit open BK channels as developed above or from inhibition by MTSET of access of paxilline to its blocking site. To further address this issue, we examined the consequences of modification of A313C by either MTSEA (Fig. 11 C) or MTSES (Fig. 11 D). Modification of A313C by the neutral MTSEA resulted in a substantive leftward shift in BK gating, but not as strong as that after modification by MTSET. After modification, the BK fractional Po at 0 mV and 10 µM Ca^{2+} was ~0.48, whereas 100 nM paxilline produced a fractional block of ~0.5. Modification of Slo1-A313C by the negatively charged MTSES resulted in a modest leftward gating shift, and inhibition by 100 nM paxilline of the modified channels (Po at equilibration conditions was ~0.12) was only slightly weaker than that for inhibition of the unmodified Slo1-A313C channels.

Although the three MTS reagents differ in net charge conferred on the modified Cys residue, they are of generally similar size. Give that paxilline is neutral at physiological pH, it seems highly unlikely that the differences among MTS moieties on the extent of paxilline inhibition reflect either electrostatic or steric hindrance of paxilline binding. On the other hand, the reduction in paxilline sensitivity of MTS-modified A313C channels provides further support for the view that inhibition by paxilline is inversely correlated with increases in channel Po.

Access of paxilline to its blocking position is hindered by compounds thought to occupy the inner pore

The ability of the G311S mutation to disrupt paxilline blockade and the key role of Slo1 S6 in inhibition by paxilline suggest that the BK channel central cavity may play a role in paxilline blockade (Zhou et al., 2010). Furthermore, the results showing that binding of a single paxilline molecule produces inhibition also suggest an action of paxilline on the axis of the permeation pathway. To further address this issue, we have asked whether compounds known to occupy the BK inner pore may hinder paxilline inhibition. We used two different tests: first, examination of the onset of paxilline inhibition in the presence of a bulky pore blocker; and second, examination of the ability of sucrose, an impermeant solute known to occupy the BK inner cavity (Brelidze and Magleby, 2005), to impede paxilline inhibition.

As a BK channel pore blocker, we used the bulky molecule N-(4-[benzoyl]benzyl)-N,N,N-tributylammonium (bbTBA), which has been shown previously to block both open and closed BK channels (Wilkens and Aldrich, 2006; Tang et al., 2009). For any pair of pore blockers, if one determines the steady-state block produced by each agent producing near half-maximal block, examination of the blocking effects of both applied together potentially allows discrimination between competitive and noncompetitive mechanisms. In fact, this was used to show that inhibition of BK channels by TBA and bbTBA occurs in a competitive fashion (Wilkens and Aldrich, 2006). However, this approach works best for rapid blockers, where onset and recovery from block allows ready determination of the fractional block under any condition. In the present case, we are coupling a faster blocker, bbTBA, with a slower blocker, paxilline. As a consequence, we chose a different strategy that takes advantage of the fact that the washout of bbTBA

will be essentially complete before any channels blocked by paxilline will have unblocked. Reasoning that channels, once blocked by paxilline, will recover from paxilline inhibition slowly, we examined whether the presence of bbTBA might reduce the fraction of channels blocked by paxilline.

We used 100 µM bbTBA, a concentration that exceeds the channel blocking affinity by ~10-fold (Wilkens and Aldrich, 2006; Tang et al., 2009). An advantage of the use of bbTBA is that it has been shown to occupy both closed and open BK channels. We then examined block by 100 nM paxilline, which is also near 10-fold the estimated affinity of block for the closed BK channel. An example of such an experiment is shown in Fig. 12. Currents were activated by voltage steps to 160 mV under equilibration conditions of 0 mV and 10 µM Ca^{2+}. 100 µM bbTBA was first applied to the patch to establish the time course of bbTBA block and unblock. 100 nM paxilline was then applied to the patch for ~40 s and then washed out. Block was incomplete but current was reduced ~80% before washout. Subsequently, 100 µM bbTBA was applied simultaneously with 100 nM paxilline for the same duration of application as with 100 nM paxilline alone. With both agents together, currents are completely blocked. However, upon washout, currents return to a level ~50% of the blocked level observed with paxilline alone, and then slowly recover with a time course characteristic of unblock from paxilline. This indicates that, in the presence of 100 µM bbTBA, the

number of channels blocked by paxilline was reduced ~50%. The fractional reduction of block is about that expected for a competitive model for each compound being applied at ~10-fold their estimated dissociation constants.

One simple interpretation of this result would be that the presence of bbTBA in the BK central cavity prevents or slows access of paxilline to its blocking position. However, it might also be considered that perhaps bbTBA reduces paxilline inhibition because the presence of bbTBA in the inner cavity mimics a BK channel open conformation, which we have shown above has reduced affinity for paxilline. We consider the latter possibility unlikely because of three factors: first, under the equilibration conditions of this experiment (0 mV, 10 µM Ca^{2+}), the BK Po is low (~0.05), such that channels are predominantly in closed states; second, under these conditions, bbTBA will occupy both open and closed channels with about equal affinity (Wilkens and Aldrich, 2006; Tang et al., 2009); and third, bbTBA has minimal ability to hinder the BK channel open-to-closed transition, so it is unlikely that it stabilizes the open conformation (Wilkens and Aldrich, 2006; Tang et al., 2009).

In our second test, we used 2 M sucrose, which has been shown to produce a marked reduction of outward potassium flux through BK channels, largely from bulk occupancy of the BK channel central cavity (Brelidze and Magleby, 2005). We first confirmed this effect of 2 M on macroscopic BK currents (Fig. 12 B), which
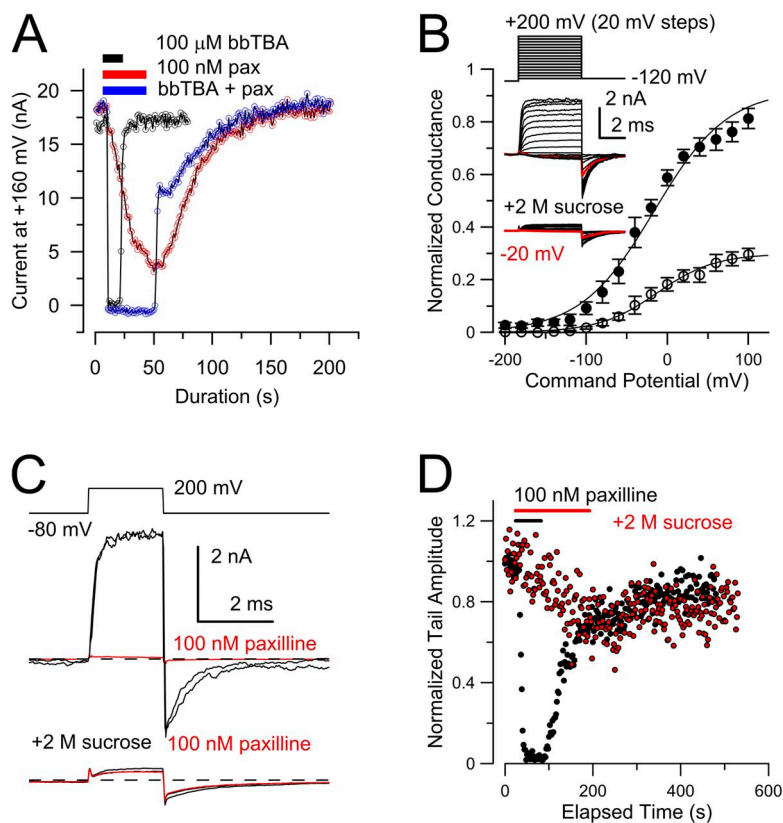
Figure 12. bbTBA and sucrose each slow paxilline inhibition. (A) Blockade of Slo1 current by 100 nM paxilline is displayed with and without simultaneous application of 100 µM bbTBA. The equilibration conditions were 0 mV with 10 µM Ca^{2+}, and BK current availability was monitored by voltage steps to 160 mV applied at 1 Hz. Blocker applications are shown with horizontal bars, with all measurements from the same patch. Block and unblock with 100 µM bbTBA alone (black) is rapid, whereas block by 100 nM paxilline (red) alone exhibits slow onset and recovery. After simultaneous application of paxilline with 100 µM bbTBA, the amount of paxilline inhibition is reduced about half. (B) BK currents were activated with 300 µM Ca^{2+} with the indicated voltage protocol without and with the addition of 2 M sucrose to the cytosolic solution. Insets show currents with a red trace at −20 mV. Sucrose markedly reduces outward current, whereas tail currents at −120 mV are reduced a little more than half. For control solutions, $V_h = −16.3 ± 7.2$ mV, whereas with 2 M sucrose, $V_h = −12.8 ± 3.3$ mV. (C) 100 nM paxilline strongly inhibits BK current, whereas in 2 M sucrose, both outward and inward currents are only slightly affected by paxilline. Top traces are single sweeps. Bottom traces correspond to an average of 15 sweeps before, during, and after washout of 100 nM paxilline. (D) Plot of time course of paxilline inhibition without and with 2 M sucrose suggests that sucrose slows the development of inhibition by paxilline.

showed that sucrose markedly suppressed outward currents, with a weaker effect on inward K⁺ current. Analysis of the tail currents monitored at −120 mV revealed little shift in the V_h of activation (Fig. 12 B). The application of 100 nM paxilline before the addition of sucrose to the cytosolic solution produced the expected robust inhibition of current, whereas with 2 M sucrose added to the cytosolic solution, only a weak inhibition of BK current was observed with paxilline (Fig. 12 C). The time course of onset of paxilline inhibition with 2 M sucrose suggests that inhibition develops more slowly in paxilline (Fig. 12 D), also consistent with the idea that the presence of sucrose in the central cavity may impede access of paxilline to its final binding position.

With the assumption that bbTBA and sucrose do not exert any effects independent of the central cavity, collectively, the bbTBA and sucrose experiments support the idea that paxilline is hindered from reaching its inhibitory position, when the central cavity is occupied by other bulky molecules.

Paxilline does not alter the ability of MTSET to modify A313C

Although the above experiments show that paxilline inhibition is hindered by bbTBA and sucrose, they do not address whether paxilline hinders inhibition by bbTBA

or inner cavity occupancy by sucrose. To address whether paxilline may hinder access of small molecules to the central cavity, we again took advantage of the ability of MTSET to modify pore residue A313C, both in open and closed states (Zhou et al., 2011). Modification of A313C by 1 mM MTSET of closed BK channels occurs with a time constant of ∼23 s and is associated with a >50% reduction in maximal conductance, as a result of effects on single-channel conductance (Zhou et al., 2011). Modification of A313C in open states is ∼200-fold more rapid. Here, because our results suggest that paxilline may only act on closed BK channels, we specifically asked whether the presence of paxilline would hinder the ability of residue A313C to be modified by MTSET when channels are closed. First, we confirmed the extent of modification of closed (−80 mV, 0 Ca²⁺) A313C channels by a 120-s application of 1 mM MTSET in the absence of paxilline (Fig. 13 A). For a time constant of 23 s, modification should be >99% complete at 120 s. The G-V curve after MTSET modification (Fig. 13 C) exhibits a substantial shift as observed previously, although less shifted than reported previously for open-state modification of A313C (Zhou et al., 2011). In separate patches, we then examined whether 500 nM paxilline hindered modification by a similar application of MTSET (Fig. 13, B and C). We found no difference in modification with or
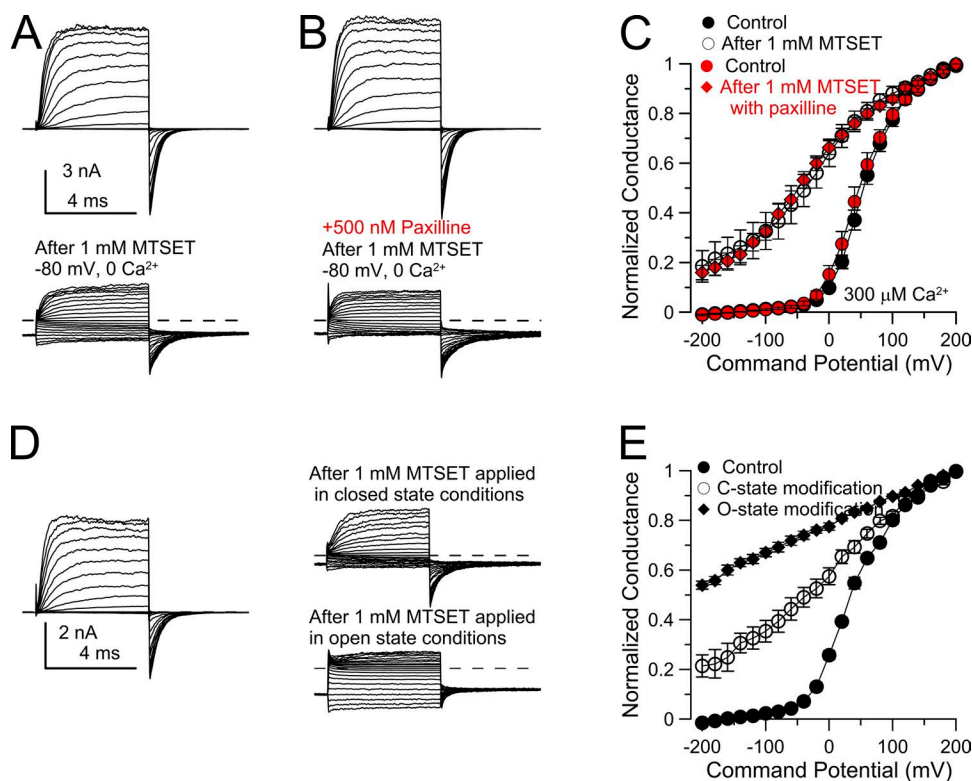
Figure 13. Paxilline does not hinder MTSET modification of A313C. (A; top) The traces show currents activated with 300 µM Ca²⁺ at voltage steps up to 200 mV for channels arising from Slo1-C430S-A313C. (Bottom) Currents were similarly elicited, but after 120 s of application of 1 mM MTSET while holding the patch at −80 mV with 0 Ca²⁺. (B; top) The traces show current for Slo1-C405A-A313C activated with 300 µM Ca²⁺. The patch was then first perfused with 500 nM paxilline for 100 s while holding at −80 mV with 0 Ca²⁺, and then exposed to 1 mM MTSET with 500 nM paxilline for 120 s while still at −80 mV with 0 Ca²⁺. (C) G-V curves summarize results from patches examined for conditions shown in A and B. Because MTSET modification was tested both without and with paxilline, two separate sets of control G-V curves at 300 µM Ca²⁺ are shown. (D) BK currents were recorded in 300 µM Ca²⁺ before (left) and after (top right) modification by

1 mM MTSET, applied for 120 s in 0 Ca²⁺ at −80 mV. Modification is similar to that in A. The patch was then held at 0 mV, 0 Ca²⁺, and then channels were opened by 20 100-msec steps to 160 mV, after which the traces on the bottom right were obtained in 300 µM Ca²⁺. (E) G-V curves correspond to conditions as in D for control, after closed-state modification by 1 mM MTSET, and then after subsequent open-state modification by the same MTSET solution.

without paxilline, although BK current was completely inhibited by paxilline during the application of MTSET. At 500 nM paxilline and a paxilline-binding constant of 10 nM, channels will be occupied by paxilline 98% of the time. If MTSET can only modify BK channels during that 2% of the time that paxilline is not present, based on the previously defined rate of MTSET modification of closed channels, essentially no modification by MTSET should be observed. This result therefore clearly shows that paxilline does not hinder MTSET modification of position A313C in closed BK channels.

Given that the partial G-V shift observed for MTSET modification of closed channels differs from the essentially constitutive activation of BK channels modified by MTSET while in open states (Zhou et al., 2011), we wondered whether the partial modification might simply reflect loss of reactive MTSET during the 120 s of MTSET application. To address this issue, a set of patches was first modified by MTSET while channels were held in closed states by bathing the patch in 0 Ca^{2+} at −80 mV (Fig. 13 D). Subsequently, the same MTSET solution was then applied while channels were held in high Po conditions. This was accomplished by changing the holding condition to 0 mV at 0 Ca^{2+} but applying 20 voltage steps to 160 mV, each of 100-ms duration. In this case, additional modification by MTSET readily occurred resulting in channels that are essentially constitutively open over a wide range of voltages, similar to the earlier observations (Zhou et al., 2011). This indicates that channels modified by MTSET while in closed states have different gating properties than those modified in open states. Using single-channel recordings, our previous work showed that two distinct step changes in single-channel current can be observed during modification of A313C by MTSET (Zhou et al., 2011), presumably corresponding to the sequential modification of at least two distinct A313C cysteines. We therefore propose that in the closed BK channel, the dimensions of the inner cavity are such that modification by only a single MTSET can be accommodated. In contrast, in the open channel, the volume allows modification at two A313C positions. The differences in the gating shifts after closed- and open-state modification reflect the effects of modification at either a single subunit or a pair of subunits. Regardless of this nuance of MTSET modification at position A313C, the important point is that wherever the position of paxilline inhibition, it does not hinder the ability of MTSET to modify at least one A313C residue.

DISCUSSION

These results describe a mechanism of inhibition of BK channels that, to our knowledge, is unique not only for BK channels but also for other K+ channels. In short,

the results suggest that the binding of small molecules to an ion channel can produce channel inhibition by stabilization of the closed-channel conformation, without any occlusion of the open-channel ion permeation pathway or effects on voltage sensors. An implication of the strong closed-state dependence of the inhibition is that the ability of paxilline to inhibit BK current among different cells will vary depending on the resting Po in a given cell. Thus, some caution may be required in the application of paxilline as a diagnostic tool for the presence of BK channels, if BK subunit composition and resting Ca^{2+} is such that the resting Po is high. Below, we consider the paxilline inhibitory mechanism within the context of other channel inhibitory mechanisms and discuss our results in terms of potential structural bases of the paxilline effects.

Categories of closed-channel block

In "open-channel block," upon channel opening, a blocking molecule simply moves from bulk solution into a position within the central axis of an ion permeation pathway that physically occludes ion permeation. In contrast, "closed-channel block" may include any of a variety of allosteric effects, often occurring in association with direct blocking effects. For many blockers for which a closed-channel block effect has been described, the underlying mechanisms remain largely unknown and, in most cases, a compound will produce both open- and closed-channel block effects.

The simplest category of closed-channel blocker is one in which the blocker is able to access a position in the closed channel that, once the channel opens, will occlude ion permeation. This might occur in either of two ways: first, lipophilic molecules may pass through hydrophobic pathways to reach a position suitable for pore occlusion, as originally proposed for uncharged local anesthetics acting on Na+ channels (Hille, 1977); and second, some channels may have a relatively accessible inner cavity allowing access of charged blocking molecules both in closed and open states, as proposed for blockade of BK channels by bulky quaternary blockers (Wilkens and Aldrich, 2006; Tang et al., 2009).

The idea that lipophilic blocking agents might access blocking sites within closed ion channels was probably first considered in classical studies of local anesthetic block of Na+ channels in the node of Ranvier (Hille, 1977). This work suggested that both charged and uncharged anesthetics reached a similar blocking position within the channel but reached the blocking site by distinct pathways: charged species required the opening of a cytosolic gate to reach a blocking position, whereas uncharged species are able to reach the same blocking position via a hydrophobic region of the protein. This idea that both categories of compounds reach similar positions within the Na+ channel aqueous cavity has recently been supported in modeling work (Bruhova

et al., 2008). More recently, it has become clear that local anesthetics may exert two types of effects on Na^+ channels: one involving allosteric effects on voltage sensors, and a second corresponding to more traditional pore occupancy and occlusion (Hanck et al., 2009; Muroi and Chanda, 2009).

For closed-channel inhibition of BK channels, bbTBA and other quaternary blockers appear to gain access to the central cavity of the pore in both open- and closed-channel conformations (Wilkens and Aldrich, 2006; Tang et al., 2009), with little difference in apparent affinities of interaction for open and closed channels. The idea that the BK central cavity is accessible in closed states has also been supported by work showing that cysteine residues introduced in the BK S6 at positions that would be expected to be inaccessible in closed Kv channels can be readily modified by charged MTS reagents, even in closed states in BK channels, albeit at rates slower than the modification of open channels (Zhou et al., 2011). The closed-channel inhibition of BK channels by bbTBA, like that of local anesthetics on Na^+ channels, represents essentially a simple pore occupancy model, with little difference in block between closed and open states.

For the two types of two cases of closed-channel block just described, both open- and closed-channel block contribute to the overall channel inhibitory effect. However, an interesting case of closed-channel block that deviates from this generality is that of tetracaine inhibition of CNG channels (Fodor et al., 1997a,b) for which the affinity of tetracaine for closed channels is ~1,000-fold stronger than for affinity to open channels. CNG channels share with BK channels the ability for molecules to enter the inner cavity in both open and closed states, allowing modification of pore-lining–introduced cysteines (Flynn and Zagotta, 2003). For inhibition by tetracaine, inhibition has been suggested to arise from a snug fit within the CNG inner cavity, but the conformational changes within the inner cavity favor binding to the closed state, but not to the open (Fodor et al., 1997a). Intriguingly, mutation of E363G, a residue presumably on the extracellular end of the CNG selectivity filter, abolishes the state dependence of tetracaine inhibition (Fodor et al., 1997a), supporting the idea that closed-state inhibition by tetracaine involves a snug positioning of tetracaine in the vicinity of the selectivity filter.

In contrast to the pore occupancy models or occlusion by toxins on the extracellular face of channels, closed-channel block by voltage-sensor toxins, such as hanatoxin (Lee et al., 2003), represents the perhaps clearest example of a compound acting at positions that are not in the axis of the ion permeation pathway, such that the inhibition of channel activation clearly must be allosteric. Given the allosteric nature of ion channel proteins, it would not be surprising if natural toxins, in particular, might have evolved to exploit other ways of stabilizing channels in closed states.

Considerations regarding the physical basis of paxilline inhibition

The paxilline inhibition of BK channels appears to exhibit features unique among previously reported closed-channel blocking effects on K^+ channels. First, the closed-channel block effects occur in the almost complete absence of open-channel block. Second, the paxilline inhibitory effect can be described by allosteric regulation of the central C-O equilibrium. Do the present results allow for any inferences regarding the physical basis for such effects? In the absence of structural information, definitive answers regarding the paxilline site of action are not possible. However, here we consider two topics: first, the route of paxilline access to its inhibitory positions; and second, the number of paxilline-binding sites on a channel.

For a lipophilic molecule like paxilline (logP = 3.62), it is natural to wonder whether paxilline reaches its position of inhibition from the paxilline reservoir in the membrane. Several results are pertinent to this topic. The ability of both the bulky pore blocker, bbTBA, and high concentrations of the impermeant solute, sucrose, to impede paxilline inhibition would seem to argue against the possibility that paxilline reaches its site of inhibition via the bulk lipid membrane. Neither bbTBA nor sucrose would be expected to impede the partitioning of paxilline into lipid or movement from lipid into channel protein. We consider it less likely that interference of bbTBA and sucrose of paxilline inhibition would arise, because of some steric effect of pore occupancy preventing lateral diffusion of paxilline through the protein into an inhibitory position.

Our measurement of the paxilline concentration dependence of inhibition of closed channels may also provide insight into the source of paxilline-mediating inhibition. We measured a forward rate of inhibition that was linear up through 2 µM paxilline with a slope of 2×10^6 $M^{-1}s^{-1}$. This is very similar to rates of open-channel block of several other ion channels, both for uncharged anesthetics (Adams, 1976) and for charged anesthetics at 0 mV (Neher and Steinbach, 1978; Lingle, 1989). For bbTBA block of BK channels, at 100 mV the forward rate of block is 1.2×10^8 $M^{-1}s^{-1}$ (Wilkens and Aldrich, 2006). Assuming a $z\delta$ of 0.148 e assigned to the forward rate, this reflects a 0-voltage forward rate of 6.7×10^7 $M^{-1}s^{-1}$. This is faster than what we observe for paxilline inhibition in closed states, but experiments examining state-dependent modification of cysteines introduced into BK S6 reveal a more than two orders of magnitude difference for MTS modification rates of residues in open versus closed channels (Zhou et al., 2011). The linearity of the rate as a function of paxilline concentration suggests that, even when channels are

largely closed, a single step, perhaps diffusionally controlled encounter appears to define the block kinetics. That this rate is comparable to what is observed for open-channel blockers suggests that it reflects block occurring from the aqueous milieu. However, does the linearity and magnitude of the blocking rate fully exclude the possibility of inhibition occurring from lipid? Linearity in the rate implies that, over this concentration range, inhibition arises from the binding of paxilline directly to the inhibitory position, whatever the source of paxilline may be. However, for paxilline reaching an inhibitory position from bulk lipid, deviation from linearity would probably be expected, if the pathway to the paxilline inhibitory position involved transient occupancy of hydrophobic pockets along the route to the binding site. Although our results do not require a particular explanation, we prefer the view that the effects of bbTBA, sucrose, and linearity in inhibition are most readily explained by paxilline inhibition occurring from the aqueous milieu.

We now address the question of the number of high affinity, closed-state paxilline-binding sites per BK channel. The concentration dependence of paxilline inhibition based on a specific allosteric model of channel inhibition (Scheme 1) suggests that inhibition arises from the binding of a single paxilline molecule to closed channels with an affinity of ~10 nM. This conclusion rests largely on the shape of the concentration–response curves at the highest Po values and highest paxilline concentrations. Schemes with multiple, identical paxilline-binding sites predict weaker inhibition at higher paxilline than we observed (Fig. 7). Based on the particular technical challenges in defining fractional inhibition at high Po and paxilline, the measures of paxilline inhibition are more likely to be underestimates than overestimates. This provides some additional confidence that the single-site model is most likely. However, one caution regarding the single-site mechanism is the possibility that, at the highest paxilline concentrations, an additional, independent paxilline inhibitory effect might occur. If that were the case, this would prevent any assertions regarding the number of identical, high affinity paxilline sites based on the Po dependence of paxilline concentration dependence.

An additional consideration relevant to this point is that, if paxilline were accessing its binding sites by coming in laterally through the protein, we would expect that up to four paxilline molecules would be able to occupy such positions simultaneously. Yet, as noted, the concentration dependence of paxilline action is best explained by the action of a single paxilline molecule. If four paxilline molecules could bind to the channel, with one being sufficient for a full inhibitory effect, this would also be consistent with the observed steady-state results. However, for recovery from inhibition, unbinding from four sites would predict a lag in the time course

of recovery from inhibition, as each of the up to four paxilline molecules must unbind before unblock occurs. This is not observed.

If the binding of a single paxilline molecule does produce BK channel inhibition, this is most consistent with a binding site that is located along the axis of the permeation pathway. In the present case, this possibility is given some support by both the bbTBA and sucrose results. A caution to this idea is the possibility that the hydrophobic bbTBA and the bulk effects of the high solution concentration with sucrose might conceivably hinder the action of a compound at other positions unrelated to their pore occupancy. However, at present, there is no precedent for such alternative effects, so the idea that bbTBA, sucrose, and paxilline interact within or in close juxtaposition to the pore would seem the most likely situation.

However, the one result that raises some question in regards to the idea of paxilline inhibition involving a single site along the axis of the permeation pathway is the failure of paxilline to prevent MTSET modification of position A313C in closed conformations. This result clearly argues against one simple view of paxilline action, namely that paxilline acts to occlude the entrance to the inner cavity, but only in the closed states (Fig. 14 A). We think it unlikely that this result can be explained by the possibility that both paxilline and MTSET might simultaneously occupy positions in the inner cavity. Overall, is there a way to reconcile the ability of bbTBA and sucrose to hinder paxilline inhibition with the lack of effect of paxilline on MTSET modification? We see no obvious simple explanation for this set of results based on our current understanding, but point to two possibilities. First, for BK, essentially nothing is known about the positioning of S6 helices as they traverse from the membrane-associated pore-gate domain to link with the appended cytosolic ligand–sensing domain. Do the cytosolic ends of the inner helices define a tightly packed funnel through which any permeant ion or blocker must pass to reach the central cavity, or is there some splayed arrangement of the cytosolic ends of the helices that may allow passage of solutes both down and between the helices to reach the central axis of the permeation pathway? In the latter case, even if a compound were to occupy a position within the tetrad of inner helices, thereby stabilizing a closed conformation, perhaps pathways for compounds to reach the inner cavity might still exist (Fig. 14 B). Assuming strict homology of the pore-gate domain of the Slo1 family of channels to Kv channels, this possibility would seem unlikely. However, many examples now exist of ways that the BK S6 helix and inner cavity differ from that of Kv channels. For example, residues that are likely to be pore facing in BK differ from those in Shaker (Chen and Aldrich, 2011; Zhou et al., 2011; Chen et al., 2014). Similarly, the pattern of modifiability of BK S6 residues differs from

that in Shaker (Zhou et al., 2011). As such, perhaps the difficulty in reconciling the bbTBA/sucrose results with the inability of paxilline to protect against MTSET modification arises from some other unusual aspect of the BK S6 and pore-gate domain that differs from the now classic Kv pore-gate domain motif. A second potential explanation is that perhaps paxilline does bind near the entrance to the closed-channel inner cavity, but in a
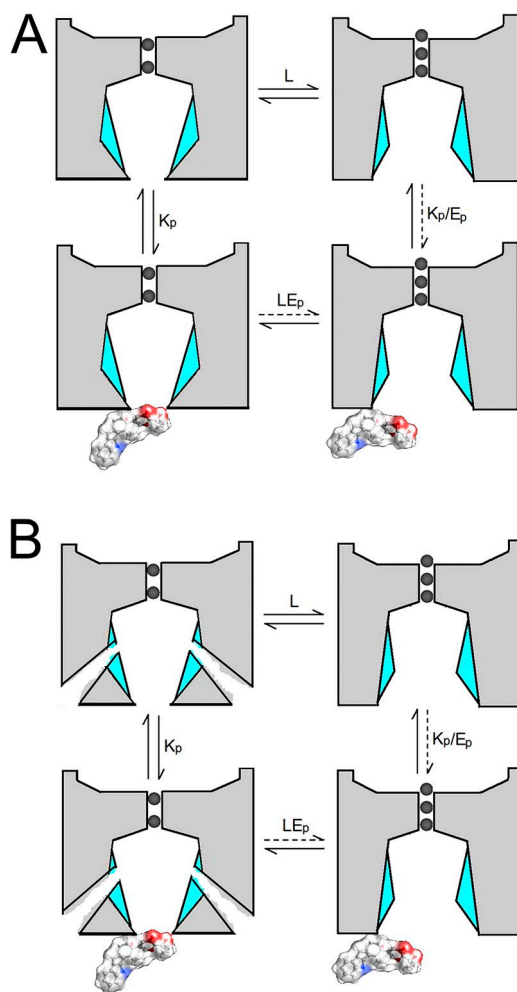
Figure 14. Cartoons describing possible views of inhibition of closed BK channels by paxilline. (A) Schematic BK channels are either closed (left pair) or open (right pair). The channels are diagrammed with an opening at the cytosolic end of the channel, which allows small molecules in and out of the inner cavity. Paxilline occludes the aperture to the inner cavity in the closed BK channel. Binding of paxilline to the closed channel (bottom left) occludes the aperture to the inner cavity. The open conformation either is unable to bind paxilline or does so with low affinity, without any occlusion of ion permeation. Dotted arrows indicate transitions that are either very low probability or do not occur. (B) Overall scheme is the same as in A, except for positions of inner-pore helices along alternative aqueous pathways for access of small molecules to the inner cavity. Thus, occlusion of the closed-channel aperture by paxilline may not impede access of small molecules to the inner cavity, such that MTS reagents can modify position A313C.

position that does not hinder MTSET access to the inner cavity. If paxilline occupied a position near the entrance to the inner cavity, bbTBA, which is perhaps large enough to fully occupy the inner cavity, may hinder paxilline movement to its blocking position. Why the smaller sucrose might also reduce paxilline inhibition is less readily explained, except perhaps by the idea that sucrose at 2 mM may simply displace a sufficient volume to reduce the effective paxilline concentration near the mouth of the channel.

The uncertainties associated with reconciliation of the bbTBA and sucrose results and absence of effect of paxilline on MTSET modification of closed states leaves open the question of whether paxilline does act along the axis of the permeation pathway. Given that paxilline can still produce inhibition in channels with MTSES-modified A313C makes it unlikely that paxilline interacts somewhere deep in the inner cavity. The failure of paxilline to hinder MTSET modification of closed states seems to argue against occlusion of the closed channels, except perhaps as modeled in Fig. 14 B, for which there is no precedent. If inhibition occurs at a position that is not on the axis of the permeation pathway, one has to consider that there may be four distinct paxilline-binding sites per channel. Yet, our analysis of the concentration dependence of paxilline inhibition supported a single-site model (Fig. 7 A). At present, our results do not allow a clear-cut answer on this point, and future functional or structural work that identifies residues likely to interact with paxilline will be required.

The role of G311 in inhibition by paxilline

The effect of mutation of G311 on paxilline sensitivity (Zhou et al., 2010) is unusual among all manipulations of BK channels we have examined. Namely, mutation of G311 is the only manipulation causing a rightward shift in BK activation at a given Ca^{2+} that is also associated with a decrease in paxilline effectiveness. This indicates that the effect of G311 mutation is not the result of state dependence, but the result of some specific change altering paxilline binding or effect. Interestingly, the pH-regulated Slo3 K^+ channel is resistant to paxilline inhibition and also lacks the corresponding hinge glycine, whereas the S300G mutation in Slo3, the hinge position, restores some paxilline sensitivity.

Is there a relationship between the ability of mutation of G311 to abolish paxilline block and the lack of block of open BK channels? G311 corresponds to a conserved glycine found in a large number of both eukaryotic and prokaryotic voltage-gated K^+ channels (Magidovich and Yifrach, 2004). Because mutations at this position alter the C-O gating equilibrium of channels where it has been studied, this glycine has been termed a "gating hinge" (Yifrach and MacKinnon, 2002; Magidovich and Yifrach, 2004), and a bend in the S6 helix has been observed at this position in K^+ channel structures (Jiang

et al., 2002a,b). An unusual aspect of BK channels is the presence of two sequential glycines, G310 and G311, which together seem likely to influence the topology of the BK S6 segment. Both the G310A and G311A mutations separately result in an ~60-mV positive shift in G-V curves at a given Ca^{2+}, whereas the double mutation shifts gating ~120 mV (Yifrach and MacKinnon, 2002). That G311 mutations result in rightward shifts in G-V curves in the BK channel, i.e., favoring a nonconducting closed channel, would seem to argue against the idea that the G311 mutation results in a more open-channel–like S6 conformation. Thus, a conservative explanation of the role of G311 is that it is essential for maintaining an S6 conformation in the closed state that is essential by paxilline block. Disruption of this critical closed-channel S6 conformation, whether by mutation of G311 or by opening the channel, abolishes paxilline block. In accordance with the proposal that paxilline may act as a closed-channel plug or to stabilize the closed-channel aperture by an interaction near the mouth of the inner cavity, G311 might result in a larger opening of this closed-channel aperture, thereby disrupting the contacts necessary for inhibition by paxilline. This can perhaps be tested via examination of MTS modification rates in closed channels containing G311A.

Implications of the state dependence of paxilline inhibition for practical usage of paxilline

It has been reported that paxilline or related alkaloids may alter the G-V curves for BK channel activation. The considerations presented here indicate that, once a given equilibration condition is established, if test steps are brief, no change in G-V will occur. However, given the slow equilibration rates, it is easy to see how under some experimental conditions apparent shifts in G-V curves might be observed. For example, for examination of BK channels, one might hold a patch at 0 mV, but then, when generating a G-V curve, briefly step to −80 mV (or more negative potentials) between test steps from −80 to 200 mV. If during paxilline application, one holds the patch at 0 mV before applying the test protocol, the block equilibrium established at 0 mV will then be altered by the new −80-mV holding level. Given the slow change in the inhibitory equilibrium, initial test steps will more reflect the equilibrium at 0 mV, whereas later steps will approach the equilibrium occurring at −80 mV. How this would exactly impact on a G-V curve would depend on the sequence of test voltages, but the point is that without maintaining the same equilibration conditions before and during a test sequence, G-V curves will be altered. Regardless of whether such an explanation may account for some earlier observations of shifts in G-V curves, it is clearly the case that protocols must take into account that the extent of paxilline inhibition depends on the Pc of the equilibration conditions. Furthermore, the specific equilibration conditions

must be clearly defined and maintained during steps that evaluate the extent of paxilline inhibition.

The state dependence of paxilline inhibition may also require caution in the use of paxilline as a tool for identification of the contributions of BK current in various cell types. An implication of the present results is that gating shifts produced by either β or γ1 subunits may reduce the effectiveness of paxilline, because of the unusual state dependence of paxilline inhibition and not because of a subunit-specific effect. Work in progress supports this idea (unpublished data). In most cases, this will probably not be a problem, as normal cell-resting potentials and normal intracellular Ca^{2+} concentrations will usually ensure that paxilline inhibition will be effective. However, if a particular stimulus paradigm results in robust cellular depolarization and Ca^{2+} elevation over tens of seconds, this may be sufficient to reverse inhibition by paxilline such that the role of BK channels may be partially obscured with particular subunit combinations.

Summary

Inhibition of BK channels by paxilline involves strong stabilization of closed conformations, with paxilline affinity for closed channels being ~1,000-fold stronger than for open channels. Various criteria suggest that paxilline reaches its blocking position from the cytosolic aqueous milieu, perhaps involving an interaction near the entrance to the inner cavity. The unusual state dependence of paxilline inhibition requires caution in the use of paxilline in cellular systems, where conditions of Po of the BK channels may not be well known.

REFERENCES

Adams, P.R. 1976. Drug blockade of open end-plate channels. *J. Physiol.* 260:531–552.

Anderson, C.S., R. MacKinnon, C. Smith, and C. Miller. 1988. Charybdotoxin block of single Ca^{2+}-activated K^+ channels. Effects of channel gating, voltage, and ionic strength. *J. Gen. Physiol.* 91:317–333. http://dx.doi.org/10.1085/jgp.91.3.317

Armstrong, C.M. 1969. Inactivation of the potassium conductance and related phenomena caused by quaternary ammonium ion injection in squid axons. *J. Gen. Physiol.* 54:553–575. http://dx.doi.org/10.1085/jgp.54.5.553

Armstrong, C.M., and B. Hille. 1972. The inner quaternary ammonium ion receptor in potassium channels of the node of Ranvier. *J. Gen. Physiol.* 59:388–400. http://dx.doi.org/10.1085/jgp.59.4.388

Banerjee, A., A. Lee, E. Campbell, and R. Mackinnon. 2013. Structure of a pore-blocking toxin in complex with a eukaryotic voltage-dependent K⁺ channel. *eLife.* 2:e00594. http://dx.doi.org/10.7554/eLife.00594

Brelidze, T.I., and K.L. Magleby. 2005. Probing the geometry of the inner vestibule of BK channels with sugars. *J. Gen. Physiol.* 126:105–121. http://dx.doi.org/10.1085/jgp.200509286

Bruhova, I., D.B. Tikhonov, and B.S. Zhorov. 2008. Access and binding of local anesthetics in the closed sodium channel. *Mol. Pharmacol.* 74:1033–1045. http://dx.doi.org/10.1124/mol.108.049759

Bush, L.P., H.H. Wilkinson, and C.L. Schardl. 1997. Bioprotective alkaloids of grass-fungal endophyte symbioses. *Plant Physiol.* 114:1–7.

Chen, X., and R.W. Aldrich. 2011. Charge substitution for a deep-pore residue reveals structural dynamics during BK channel gating. *J. Gen. Physiol.* 138:137–154. http://dx.doi.org/10.1085/jgp.201110632

Chen, X., J. Yan, and R.W. Aldrich. 2014. BK channel opening involves side-chain reorientation of multiple deep-pore residues. *Proc. Natl. Acad. Sci. USA.* 111:E79–E88. http://dx.doi.org/10.1073/pnas.1321697111

Choi, K.L., R.W. Aldrich, and G. Yellen. 1991. Tetraethylammonium blockade distinguishes two inactivation mechanisms in voltage-activated K⁺ channels. *Proc. Natl. Acad. Sci. USA.* 88:5092–5095. http://dx.doi.org/10.1073/pnas.88.12.5092

Choi, K.L., C. Mossman, J. Aubé, and G. Yellen. 1993. The internal quaternary ammonium receptor site of Shaker potassium channels. *Neuron.* 10:533–541. http://dx.doi.org/10.1016/0896-6273(93)90340-W

Cole, R., and R. Cox. 1981. Handbook of Toxic Fungal Metabolites. Academic Press, New York. 936 pp.

DiChiara, T.J., and P.H. Reinhart. 1997. Redox modulation of hslo Ca²⁺-activated K⁺ channels. *J. Neurosci.* 17:4942–4955.

Doyle, D.A., J. Morais Cabral, R.A. Pfuetzner, A. Kuo, J.M. Gulbis, S.L. Cohen, B.T. Chait, and R. MacKinnon. 1998. The structure of the potassium channel: Molecular basis of K⁺ conduction and selectivity. *Science.* 280:69–77. http://dx.doi.org/10.1126/science.280.5360.69

Essin, K., M. Gollasch, S. Rolle, P. Weissgerber, M. Sausbier, E. Bohn, I.B. Autenrieth, P. Ruth, F.C. Luft, W.M. Nauseef, and R. Kettritz. 2009. BK channels in innate immune functions of neutrophils and macrophages. *Blood.* 113:1326–1331. http://dx.doi.org/10.1182/blood-2008-07-166660

Flynn, G.E., and W.N. Zagotta. 2003. A cysteine scan of the inner vestibule of cyclic nucleotide–gated channels reveals architecture and rearrangement of the pore. *J. Gen. Physiol.* 121:563–583. http://dx.doi.org/10.1085/jgp.200308819

Fodor, A.A., K.D. Black, and W.N. Zagotta. 1997a. Tetracaine reports a conformational change in the pore of cyclic nucleotide–gated channels. *J. Gen. Physiol.* 110:591–600. http://dx.doi.org/10.1085/jgp.110.5.591

Fodor, A.A., S.E. Gordon, and W.N. Zagotta. 1997b. Mechanism of tetracaine block of cyclic nucleotide–gated channels. *J. Gen. Physiol.* 109:3–14. http://dx.doi.org/10.1085/jgp.109.1.3

Gross, A., and R. MacKinnon. 1996. Agitoxin footprinting the shaker potassium channel pore. *Neuron.* 16:399–406. http://dx.doi.org/10.1016/S0896-6273(00)80057-4

Han, T.S., R.W. Teichert, B.M. Olivera, and G. Bulaj. 2008. Conus venoms—a rich source of peptide-based therapeutics. *Curr. Pharm. Des.* 14:2462–2479. http://dx.doi.org/10.2174/138161208785777469

Hanck, D.A., E. Nikitina, M.M. McNulty, H.A. Fozzard, G.M. Lipkind, and M.F. Sheets. 2009. Using lidocaine and benzocaine to link sodium channel molecular conformations to state-dependent antiarrhythmic drug affinity. *Circ. Res.* 105:492–499. http://dx.doi.org/10.1161/CIRCRESAHA.109.198572

Hille, B. 1977. Local anesthetics: hydrophilic and hydrophobic pathways for the drug-receptor reaction. *J. Gen. Physiol.* 69:497–515. http://dx.doi.org/10.1085/jgp.69.4.497

Horrigan, F.T., and R.W. Aldrich. 1999. Allosteric voltage gating of potassium channels II. Mslo channel gating charge movement in the absence of Ca²⁺. *J. Gen. Physiol.* 114:305–336. http://dx.doi.org/10.1085/jgp.114.2.305

Horrigan, F.T., and R.W. Aldrich. 2002. Coupling between voltage sensor activation, Ca²⁺ binding and channel opening in large conductance (BK) potassium channels. *J. Gen. Physiol.* 120:267–305. http://dx.doi.org/10.1085/jgp.20028605

Imlach, W.L., S.C. Finch, J. Dunlop, and J.E. Dalziel. 2009. Structural determinants of lolitrems for inhibition of BK large conductance Ca²⁺-activated K⁺ channels. *Eur. J. Pharmacol.* 605:36–45. http://dx.doi.org/10.1016/j.ejphar.2008.12.031

Imlach, W.L., S.C. Finch, Y. Zhang, J. Dunlop, and J.E. Dalziel. 2011. Mechanism of action of lolitrem B, a fungal endophyte derived toxin that inhibits BK large conductance Ca²⁺-activated K⁺ channels. *Toxicon.* 57:686–694. http://dx.doi.org/10.1016/j.toxicon.2011.01.013

Jiang, Y., A. Lee, J. Chen, M. Cadene, B.T. Chait, and R. MacKinnon. 2002a. Crystal structure and mechanism of a calcium-gated potassium channel. *Nature.* 417:515–522. http://dx.doi.org/10.1038/417515a

Jiang, Y., A. Lee, J. Chen, M. Cadene, B.T. Chait, and R. MacKinnon. 2002b. The open pore conformation of potassium channels. *Nature.* 417:523–526. http://dx.doi.org/10.1038/417523a

Knaus, H.G., O.B. McManus, S.H. Lee, W.A. Schmalhofer, M. Garcia-Calvo, L.M. Helms, M. Sanchez, K. Giangiacomo, J.P. Reuben, A.B. Smith III, et al. 1994. Tremorgenic indole alkaloids potently inhibit smooth muscle high-conductance calcium-activated potassium channels. *Biochemistry.* 33:5819–5828. http://dx.doi.org/10.1021/bi00185a021

Lee, H.C., J.M. Wang, and K.J. Swartz. 2003. Interaction between extracellular Hanatoxin and the resting conformation of the voltage-sensor paddle in Kv channels. *Neuron.* 40:527–536. http://dx.doi.org/10.1016/S0896-6273(03)00636-6

Lee, S.Y., and R. MacKinnon. 2004. A membrane-access mechanism of ion channel inhibition by voltage sensor toxins from spider venom. *Nature.* 430:232–235. http://dx.doi.org/10.1038/nature02632

Lenaeus, M.J., M. Vamvouka, P.J. Focia, and A. Gross. 2005. Structural basis of TEA blockade in a model potassium channel. *Nat. Struct. Mol. Biol.* 12:454–459. http://dx.doi.org/10.1038/nsmb929

Liang, S. 2008. Proteome and peptidome profiling of spider venoms. *Expert Rev. Proteomics.* 5:731–746. http://dx.doi.org/10.1586/14789450.5.5.731

Lingle, C.J. 1989. Anomalous voltage dependence of channel blockade at a crustacean glutamate-mediated synapse. *J. Physiol.* 409:403–430.

Long, S.B., E.B. Campbell, and R. Mackinnon. 2005. Crystal structure of a mammalian voltage-dependent Shaker family K⁺ channel. *Science.* 309:897–903. http://dx.doi.org/10.1126/science.1116269

MacKinnon, R., and C. Miller. 1988. Mechanism of charybdotoxin block of the high-conductance, Ca²⁺-activated K⁺ channel. *J. Gen. Physiol.* 91:335–349. http://dx.doi.org/10.1085/jgp.91.3.335

Magidovich, E., and O. Yifrach. 2004. Conserved gating hinge in ligand- and voltage-dependent K⁺ channels. *Biochemistry.* 43:13242–13247. http://dx.doi.org/10.1021/bi048377v

Meera, P., M. Wallner, and L. Toro. 2000. A neuronal beta subunit (KCNMB4) makes the large conductance, voltage- and Ca²⁺-activated K⁺ channel resistant to charybdotoxin and iberiotoxin.

Proc. Natl. Acad. Sci. USA. 97:5562–5567. http://dx.doi.org/10 .1073/pnas.100118597

Milescu, M., F. Bosmans, S. Lee, A.A. Alabi, J.I. Kim, and K.J. Swartz. 2009. Interactions between lipids and voltage sensor paddles detected with tarantula toxins. *Nat. Struct. Mol. Biol.* 16:1080–1085. http://dx.doi.org/10.1038/nsmb.1679

Muroi, Y., and B. Chanda. 2009. Local anesthetics disrupt energetic coupling between the voltage-sensing segments of a sodium channel. *J. Gen. Physiol.* 133:1–15. http://dx.doi.org/10.1085/ jgp.200810103

Narahashi, T., J.W. Moore, and W.R. Scott. 1964. Tetrodotoxin blockage of sodium conductance increase in lobster giant axons. *J. Gen. Physiol.* 47:965–974. http://dx.doi.org/10.1085/jgp.47.5.965

Narahashi, T., J.W. Moore, and R.N. Poston. 1967. Tetrodotoxin derivatives: Chemical structure and blockage of nerve membrane conductance. *Science.* 156:976–979. http://dx.doi.org/10.1126/ science.156.3777.976

Neher, E., and J.H. Steinbach. 1978. Local anaesthetics transiently block currents through single acetylcholine-receptor channels. *J. Physiol.* 277:153–176.

Perozo, E., D.M. Cortes, and L.G. Cuello. 1999. Structural rearrangements underlying K+-channel activation gating. *Science.* 285:73–78. http://dx.doi.org/10.1126/science.285.5424.73

Raffaelli, G., C. Saviane, M.H. Mohajerani, P. Pedarzani, and E. Cherubini. 2004. BK potassium channels control transmitter release at CA3-CA3 synapses in the rat hippocampus. *J. Physiol.* 557:147–157. http://dx.doi.org/10.1113/jphysiol.2004.062661

Sanchez, M., and O.B. McManus. 1996. Paxilline inhibition of the alpha-subunit of the high-conductance calcium-activated potassium channel. *Neuropharmacology.* 35:963–968. http://dx.doi.org/ 10.1016/0028-3908(96)00137-2

Shao, L.R., R. Halvorsrud, L. Borg-Graham, and J.F. Storm. 1999. The role of BK-type Ca2+-dependent K+ channels in spike broadening during repetitive firing in rat hippocampal pyramidal cells. *J. Physiol.* 521:135–146. http://dx.doi.org/10.1111/j.1469-7793.1999.00135.x

Smith, C., M. Phillips, and C. Miller. 1986. Purification of charybdotoxin, a specific inhibitor of the high-conductance Ca2+-activated K+ channel. *J. Biol. Chem.* 261:14607–14613.

Swartz, K.J., and R. MacKinnon. 1997a. Hanatoxin modifies the gating of a voltage-dependent K+ channel through multiple binding sites. *Neuron.* 18:665–673. http://dx.doi.org/10.1016/S0896-6273 (00)80306-2

Swartz, K.J., and R. MacKinnon. 1997b. Mapping the receptor site for hanatoxin, a gating modifier of voltage-dependent K+ channels. *Neuron.* 18:675–682. http://dx.doi.org/10.1016/S0896-6273(00)80307-4

Tammaro, P., A.L. Smith, S.R. Hutchings, and S.V. Smirnov. 2004. Pharmacological evidence for a key role of voltage-gated K+ channels in the function of rat aortic smooth muscle cells.

Br. J. Pharmacol. 143:303–317. http://dx.doi.org/10.1038/sj.bjp .0705957

Tang, Q.Y., X.-H. Zeng, and C.J. Lingle. 2009. Closed-channel block of BK potassium channels by bbTBA requires partial activation. *J. Gen. Physiol.* 134:409–436. http://dx.doi.org/10.1085/ jgp.200910251

Uysal, S., V. Vásquez, V. Tereshko, K. Esaki, F.A. Fellouse, S.S. Sidhu, S. Koide, E. Perozo, and A. Kossiakoff. 2009. Crystal structure of full-length KcsA in its closed conformation. *Proc. Natl. Acad. Sci. USA.* 106:6644–6649. http://dx.doi.org/10.1073/ pnas.0810663106

Wang, J., V. Yarov-Yarovoy, R. Kahn, D. Gordon, M. Gurevitz, T. Scheuer, and W.A. Catterall. 2011. Mapping the receptor site for α-scorpion toxins on a Na+ channel voltage sensor. *Proc. Natl. Acad. Sci. USA.* 108:15426–15431. http://dx.doi.org/10.1073/ pnas.1112320108

Wilkens, C.M., and R.W. Aldrich. 2006. State-independent block of BK channels by an intracellular quaternary ammonium. *J. Gen. Physiol.* 128:347–364. http://dx.doi.org/10.1085/jgp.200609579

Xia, X.-M., J.P. Ding, and C.J. Lingle. 1999. Molecular basis for the inactivation of Ca2+- and voltage-dependent BK channels in adrenal chromaffin cells and rat insulinoma tumor cells. *J. Neurosci.* 19:5255–5264.

Xia, X.-M., J.-P. Ding, X.-H. Zeng, K.-L. Duan, and C.J. Lingle. 2000. Rectification and rapid activation at low Ca2+ of Ca2+-activated, voltage-dependent BK currents: Consequences of rapid inactivation by a novel β subunit. *J. Neurosci.* 20:4890–4903.

Yifrach, O., and R. MacKinnon. 2002. Energetics of pore opening in a voltage-gated K+ channel. *Cell.* 111:231–239. http://dx.doi .org/10.1016/S0092-8674(02)01013-9

Zhang, G., and F.T. Horrigan. 2005. Cysteine modification alters voltage- and Ca2+-dependent gating of large conductance (BK) potassium channels. *J. Gen. Physiol.* 125:213–236. http://dx.doi .org/10.1085/jgp.200409149

Zhang, X., C.R. Solaro, and C.J. Lingle. 2001. Allosteric regulation of BK channel gating by Ca2+ and Mg2+ through a nonselective, low affinity divalent cation site. *J. Gen. Physiol.* 118:607–636. http://dx.doi.org/10.1085/jgp.118.5.607

Zhou, M., J.H. Morais-Cabral, S. Mann, and R. MacKinnon. 2001. Potassium channel receptor site for the inactivation gate and quaternary amine inhibitors. *Nature.* 411:657–661. http://dx.doi .org/10.1038/35079500

Zhou, Y., Q.Y. Tang, X.-M. Xia, and C.J. Lingle. 2010. Glycine311, a determinant of paxilline block in BK channels: A novel bend in the BK S6 helix. *J. Gen. Physiol.* 135:481–494. http://dx.doi .org/10.1085/jgp.201010403

Zhou, Y., X.M. Xia, and C.J. Lingle. 2011. Cysteine scanning and modification reveal major differences between BK channels and Kv channels in the inner pore region. *Proc. Natl. Acad. Sci. USA.* 108:12161–12166. http://dx.doi.org/10.1073/pnas.1104150108